

AD-A035 855

GEORGIA INST OF TECH ATLANTA

F/G 9/5

COMPUTATIONAL TECHNIQUES FOR THE REDUCTION OF NONLINEAR EFFECTS--ETC(U)

DEC 76 K L SU

F30602-75-C-0118

UNCLASSIFIED

RADC-TR-76-369

NL

1 OF 2  
AD-A  
035 855



U.S. DEPARTMENT OF COMMERCE  
National Technical Information Service

AD-A035 855

COMPUTATIONAL TECHNIQUES FOR THE REDUCTION  
OF NONLINEAR EFFECTS USING PASSIVE  
COMPENSATING NETWORKS

GEORGIA INSTITUTE OF TECHNOLOGY  
ATLANTA, GEORGIA

DECEMBER 1976

ADA 035855

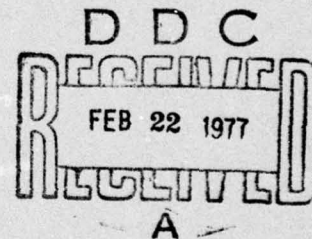
RADC-TR-76-369  
Technical Report  
December 1976



COMPUTATIONAL TECHNIQUES FOR THE REDUCTION OF NONLINEAR  
EFFECTS USING PASSIVE COMPENSATING NETWORKS

Georgia Institute of Technology

Approved for public release;  
distribution unlimited.



**ROME AIR DEVELOPMENT CENTER  
AIR FORCE SYSTEMS COMMAND  
GRIFFISS AIR FORCE BASE, NEW YORK 13441**

Copy available to DDC does not  
permit fully legible reproduction

REPRODUCED BY  
**NATIONAL TECHNICAL  
INFORMATION SERVICE**  
U. S. DEPARTMENT OF COMMERCE  
SPRINGFIELD, VA. 22161



This report has been reviewed by the RADC Information Office (OI) and is releasable to the National Technical Information Service (NTIS). At NTIS it will be releasable to the general public, including foreign nations.

This report has been reviewed and approved for publication.

APPROVED:

*Daniel E. Warren*

DANIEL E. WARREN  
Project Engineer

APPROVED:

*Joseph J. Naresky*

JOSEPH J. NARESKY  
Chief, Reliability & Compatibility Division

FOR THE COMMANDER:

*John P. Huss*

JOHN P. HUSS  
Acting Chief, Plans Office

ACCESSION	
NTIS	WFO 1000
DOC	DOI 1000
UNCLASSIFIED	
JUSTIFICATION	
BY	
DISTRIBUTION	
Dist.	
A	

Do not return this copy. Retain or destroy.

i(A)



UNCLASSIFIED

SECURITY CLASSIFICATION OF THIS PAGE (When Data Entered)

REPORT DOCUMENTATION PAGE		READ INSTRUCTIONS BEFORE COMPLETING FORM
1. REPORT NUMBER RADG-TR-76-369	2. GOVT ACCESSION NO.	3. RECIPIENT'S CATALOG NUMBER
4. TITLE (and Subtitle) COMPUTATIONAL TECHNIQUES FOR THE REDUCTION OF NONLINEAR EFFECTS USING PASSIVE COMPENSATING NETWORKS		5. TYPE OF REPORT & PERIOD COVERED Phase Report 1 Oct 74 - 1 Jul 76
		6. PERFORMING ORG. REPORT NUMBER N/A
7. AUTHOR(s) Kendall L. Su		8. CONTRACT OR GRANT NUMBER(s) F30602-75-C-0118
9. PERFORMING ORGANIZATION NAME AND ADDRESS Georgia Institute of Technology Atlanta GA 30332		10. PROGRAM ELEMENT, PROJECT, TASK AREA & WORK UNIT NUMBERS 45400259
11. CONTROLLING OFFICE NAME AND ADDRESS Rome Air Development Center (RBCT) Griffiss AFB NY 13441		12. REPORT DATE December 1976
		13. NUMBER OF PAGES 86
14. MONITORING AGENCY NAME & ADDRESS (if different from Controlling Office) Same		15. SECURITY CLASS. (of this report) UNCLASSIFIED
		15a. DECLASSIFICATION/DOWNGRADING SCHEDULE N/A
16. DISTRIBUTION STATEMENT (of this Report)  Approved for public release; distribution unlimited.		
17. DISTRIBUTION STATEMENT (of the abstract entered in Block 20, if different from Report) Same		
18. SUPPLEMENTARY NOTES RADG Project Engineer: Daniel E. Warren (RBCT)		
19. KEY WORDS (Continue on reverse side if necessary and identify by block number) Nonlinear Circuit Analysis Interference Electromagnetic Compatibility Nonlinear Effects		
20. ABSTRACT (Continue on reverse side if necessary, and identify by block number) The objective of this effort is to develop design procedures to minimize nonlinear effects in mildly nonlinear circuits. Specifically, design procedures that will reduce nonlinear distortions such as intermodulation, desensitization, gain compression, etc. in communication equipment. The approach used relies on reducing in-band nonlinear distortion products by modifying the first order transfer functions outside the band of interest. The technique makes use of the fact that certain high-order nonlinear effects in the passband are functions of first-order network parameters at frequencies outside the band. By		

DD FORM 1 JAN 73 1473 EDITION OF 1 NOV 65 IS OBSOLETE

UNCLASSIFIED

SECURITY CLASSIFICATION OF THIS PAGE (When Data Entered)

Copy available to DDC does not  
 permit fully legible reproduction

UNCLASSIFIED

SECURITY CLASSIFICATION OF THIS PAGE(When Data Entered)

appropriate modification of these first-order parameters in-band, nonlinear effects can be reduced.

UNCLASSIFIED

SECURITY CLASSIFICATION OF THIS PAGE(When Data Entered)

$i(a)$

$f_1$  (MHz)

## PREFACE

The RADC Post-Doctoral Program is a cooperative venture between RADC and some sixty-five universities eligible to participate in the program. Syracuse University (Department of Electrical and Computer Engineering), Purdue University (School of Electrical Engineering), Georgia Institute of Technology (School of Electrical Engineering), and State University of New York at Buffalo (Department of Electrical Engineering) act as prime contractor schools with other schools participating via sub-contracts with the prime schools. The U.S. Air Force Academy (Department of Electrical Engineering), Air Force Institute of Technology (Department of Electrical Engineering), and the Naval Post Graduate School (Department of Electrical Engineering) also participate in the program.

The Post-Doctoral Program provides an opportunity for faculty at participating universities to spend up to one year full time on exploratory development and problem-solving efforts with the post-doctorals splitting their time between the customer location and their educational institutions. The program is totally customer-funded with current projects being undertaken for Rome Air Development Center (RADC), Space and Missile Systems Organization (SAMSO), Aeronautical Systems Division (ASD), Electronic Systems Division (ESD), Air Force Avionics Laboratory (AFAL), Foreign Technology Division (FTD), Air Force Weapons Laboratory (AFWL), Armament Development and Test Center (ADTC), Air Force Communications Service



(AFCS), Aerospace Defense Command (ADC), Hq USAF, Defense Communications Agency (DCA), Navy, Army, Aerospace Medical Division (AMD), and Federal Aviation Administration (FAA).

Further information about the RADC Post-Doctoral Program can be obtained from Jacob Scherer, RADC, tel. AV 587-2543, COMM (315)-330-2543.

This effort was conducted by Kendall L. Su of Georgia Institute of Technology under the sponsorship of the Rome Air Development Center Post-Doctoral Program for the Computability Techniques Section. Daniel E. Warren of RADC/RBCT was the task project engineer and provided overall technical direction with assistance from Carmen A. Paludi, Jr. (RADC/RBCT) and Dr. James J. Whalen (State University of New York at Buffalo).

#### ACKNOWLEDGMENTS

The author is deeply indebted to Mr. John F. Spina of RADC for his continual assistance and invaluable technical consultation throughout the duration of this investigation. His encouragement provided the author with the motivation to venture into an area which was largely unexplored.

Special appreciation is also extended to Dr. Donald Weiner of Syracuse University for sharing his experience in this general area, for his help in explaining certain difficulties, for his general assistance in charting the course of this study, and for his comments on this report.

The careful reading of the draft of this report by Messrs. Carmen A. Paludi, Jr., Daniel E. Warren, and Daniel Kenneally of RADC is also gratefully acknowledged.

The supporting effort in computer programming was carried out by Messrs. David Yu and Sam Lau of Georgia Tech.

# TABLE OF CONTENTS

	Page
PREFACE	i
ACKNOWLEDGMENTS	iii
TABLE OF CONTENTS	iv
LIST OF FIGURES	vi
CHAPTER I INTRODUCTION	1
CHAPTER II BROADBAND INTERMODULATION REDUCTION WITH EMITTER RESISTANCE NONLINEARITY ONLY	2
2.1 The Amplifier	2
2.2 The Interference Problem	4
2.3 The Compensating Network	6
2.4 Relationship in the Equivalent Circuit of the Amplifier	9
2.5 The Optimization Program	11
2.6 Third-Order Intermodulation of the Amplifier	12
2.7 Maximum Average Reduction at the Four Vertexes of the Parallelogram	12
2.8 Maximum Average Reduction Along the Border	17
2.9 Maximum-Minimum Reduction Along the Border	18
2.10 Minimum Maximum $ H_3 $	18
2.11 Additions of $Y_1$	24
2.12 Two Separate Networks for High-Frequency and Low-Frequency Compensation	28
2.13 The Search for an Idealized Compensating Network	30
2.14 Conclusions and Conjectures	37



CHAPTER III	MEDIUM TO NARROW BAND INTERMODULATION REDUCTION WITH EMITTER RESISTANCE NON- LINEARITY ONLY	40
3.1	Introduction	40
3.2	The Frequency Specification	40
3.3	Bandwidth and Reduction Trade-Off	41
3.4	Third-Order Intermodulation Reduction Achievable Using Two Compensating Networks	46
3.5	Third-Order Intermodulation Reduction Achievable Using Four Compensating Networks	49
CHAPTER IV	OTHER TRANSISTOR NONLINEARITIES	52
4.1	Introduction	52
4.2	Transistor Nonlinearities	52
4.3	Numerical Experimentation Including Other Nonlinearities	60
CHAPTER V	COMPUTATION OF COMPENSATING NETWORK PARAMETERS	64
5.1	Introduction	64
5.2	Calculation of Third-Order Intermodulation	65
5.3	Interactive Mode Search for Values of $Y_1$ and $Y_3$ at One Frequency Combination	70
5.4	Automatic Research for Values of $Y_1$ and $Y_3$ at one Frequency Combination	73
5.5	Automatic Search for Maximum Reduction Over a Region of Frequency Combinations	76
CHAPTER VI	SUMMARY	81
REFERENCES		83
APPENDIX A	DESCRIPTION OF SUBROUTINE CGJR	84

# LIST OF FIGURES

	Page
Fig. 2.1 A common-emitter tuned amplifier	3
Fig. 2.2 Equivalent circuit of the transmitter	3
Fig. 2.3 Linear amplifier response without compensation	5
Fig. 2.4 Frequency combinations that produce third-order intermodulation in the IF band	7
Fig. 2.5 Common-emitter amplifier with a compensating network $Y_3$	8
Fig. 2.6 Equivalent circuit of the common-emitter amplifier of Fig. 2.5	10
Fig. 2.7 Network to give the admittance of (2.5) with coefficients given in (2.11)	14
Fig. 2.8 Relative third-order transfer functions along the border of the frequency parallelogram when the average reduction at the vertexes is maximized	16
Fig. 2.9 Network to give $Y_3$ of (2.5) with coefficients given in (2.12)	17
Fig. 2.10 Relative third-order transfer functions along the border of the frequency parallelogram when the average reduction along the border is maximized	20
Fig. 2.11 Relative third-order transfer functions along the border of the frequency parallelogram when the minimum reduction along the border is maximized	22
Fig. 2.12 Network to give $Y_3$ of (2.5) with coefficients given in (2.13)	23
Fig. 2.13 Relative third-order transfer function along the border of the frequency parallelogram when the maximum of $ H_3 $ along the border is maximized	26
Fig. 2.14 Amplifier with two compensating networks, $Y_1$ and $Y_3$	27

Fig. 2.15	Amplifier with four compensating networks	29
Fig. 2.16a	Ideal (solid) and approximate (dashed) $Y_{1\ hi}$	32
Fig. 2.16b	Ideal $Y_{3\ hi}$	33
Fig. 2.16c	Ideal $Y_{1\ lo}$	34
Fig. 2.16d	Ideal (solid) and approximate (dashed) $Y_{1\ lo}$	35
Fig. 2.17	Networks with admittances approximating those of Figure 2.16a and d	36
Fig. 3.1	Frequency regions of interest	42
Fig. 3.2	Frequency regions used in the study of bandwidth and reduction trade-off	43
Fig. 3.3	Amplifier with two compensating networks, one for each frequency range	44
Fig. 3.4	Frequency combinations of point designations	47
Fig. 3.5	Amplifier with four compensating networks	49
Fig. 4.1	Amplifier circuit with transistor equivalent circuit including all known nonlinearities	53



## CHAPTER I

### INTRODUCTION

In a previous study [1,2,3], it was shown that certain in-band higher-order nonlinear effects in a transistor amplifier can be reduced by modifying its out-of-band linear or first-order response. In particular, it was demonstrated that the third-order intermodulation in the pass band produced by two signals whose frequencies are also in the pass band can be eliminated by modifying the linear response of the amplifier at two frequencies outside the pass band.

This report summarizes the extension of that study in two directions. First, the extent to which this technique can be applied to signals whose frequencies fall within certain ranges will be investigated. Second, a study of the effects of the various transistor nonlinearities on the required compensating networks will be investigated.

The major part of this work is done in the mode of numerical experimentation. This method is chosen primarily because of the fact that the relationship which governs the effects of linear response on the intermodulation is too complex to lend itself to theoretical derivations. Even if the latter were feasible, it would still be desirable to ascertain in advance the likelihood of its success before a major effort is launched to obtain general results. The numerical result obtained here would also be helpful in guiding the laboratory experimental work that is visualized in the future to verify the applicability of this new approach to the problem of reducing the distortion due to nonlinearities in active circuits.

## CHAPTER II

### BROADBAND INTERMODULATION REDUCTION WITH EMITTER RESISTANCE NONLINEARITY ONLY

#### 2.1 The Amplifier

As the first numerical experimentation, the amplifier of Figure 2.1 is used. This amplifier is a modification of the amplifier used in Reference 1, 2, and 3.

The amplifier is a common-emitter amplifier with a tuned load to produce a band-pass characteristic. Both the load resistor and the source resistor,  $R_s$  and  $R_L$ , are  $75\Omega$  each. The transistor is a Western Electric Type A2436 whose equivalent circuit is given in Figure 2.2 and the circuit parameters are given below:

$$\begin{aligned}C_1 &= 5 \times 10^{-12} \text{ F} & C_2 &= 1.5 \times 10^{-9} \text{ F} \\C_3 &= 9.2 \times 10^{-12} \text{ F} & r_b &= 13.6\Omega \\r_c &= 5200\Omega & \alpha &= 0.992035\end{aligned}$$

The emitter resistor ( $r_e$ ) is assumed to be nonlinear and has the voltage-current relationship

$$i_e = \Psi(e_{be}) = k_1 e_{be} + k_2 e_{be}^2 + k_3 e_{be}^3$$

with

$$k_1 = \frac{1}{r_e} = 4.6189 \text{ A/V}$$

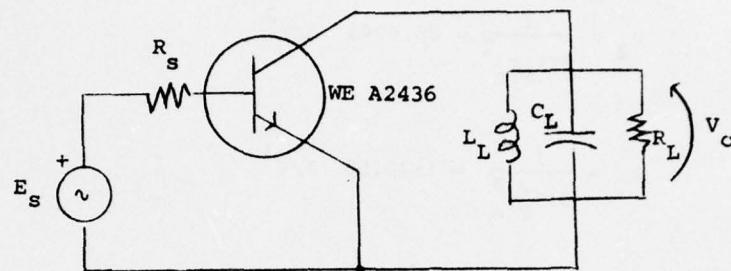


FIGURE 2.1. A Common-Emitter Tuned Amplifier

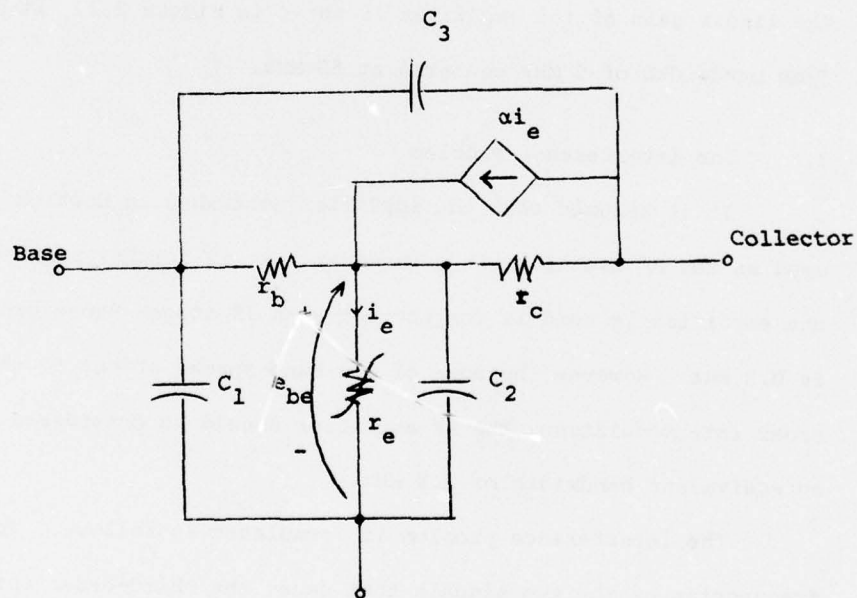


FIGURE 2.2. Equivalent Circuit of the Transistor.



The transistor is biased at the emitter current  $I_E = 0.12A$ . We assume

$$k_2 = \frac{1}{2I_E r_e^2} = 88.8941 \text{ A/V}^2$$

$$k_3 = \frac{1}{3I_E^2 r_e^3} = 1140.55 \text{ A/V}^3$$

The load tuning circuit has

$$L_L = 8.5262 \text{ nH}$$

$$C_L = 1.1884 \text{ nF}$$

The linear gain of the amplifier is shown in Figure 2.3. It has a 3-dB bandwidth of 5 MHz centered at 50 MHz.

## 2.2 The Interference Problem

It is assumed that the amplifier described in Section 2.1 is used as the RF amplifier in a receiver. It is further assumed that the amplifier is used in conjunction with IF stages whose bandwidth is 0.5 MHz. However, because of the band-spread effect of the third-order intermodulation, the IF amplifier should be considered to have an equivalent bandwidth of 1.5 MHz.

The interference problem is formulated as follows. The frequencies of the two signals that cause the third-order intermodulation are designated  $f_1$  and  $f_2$ . They fall within the following constraints (in MHz):

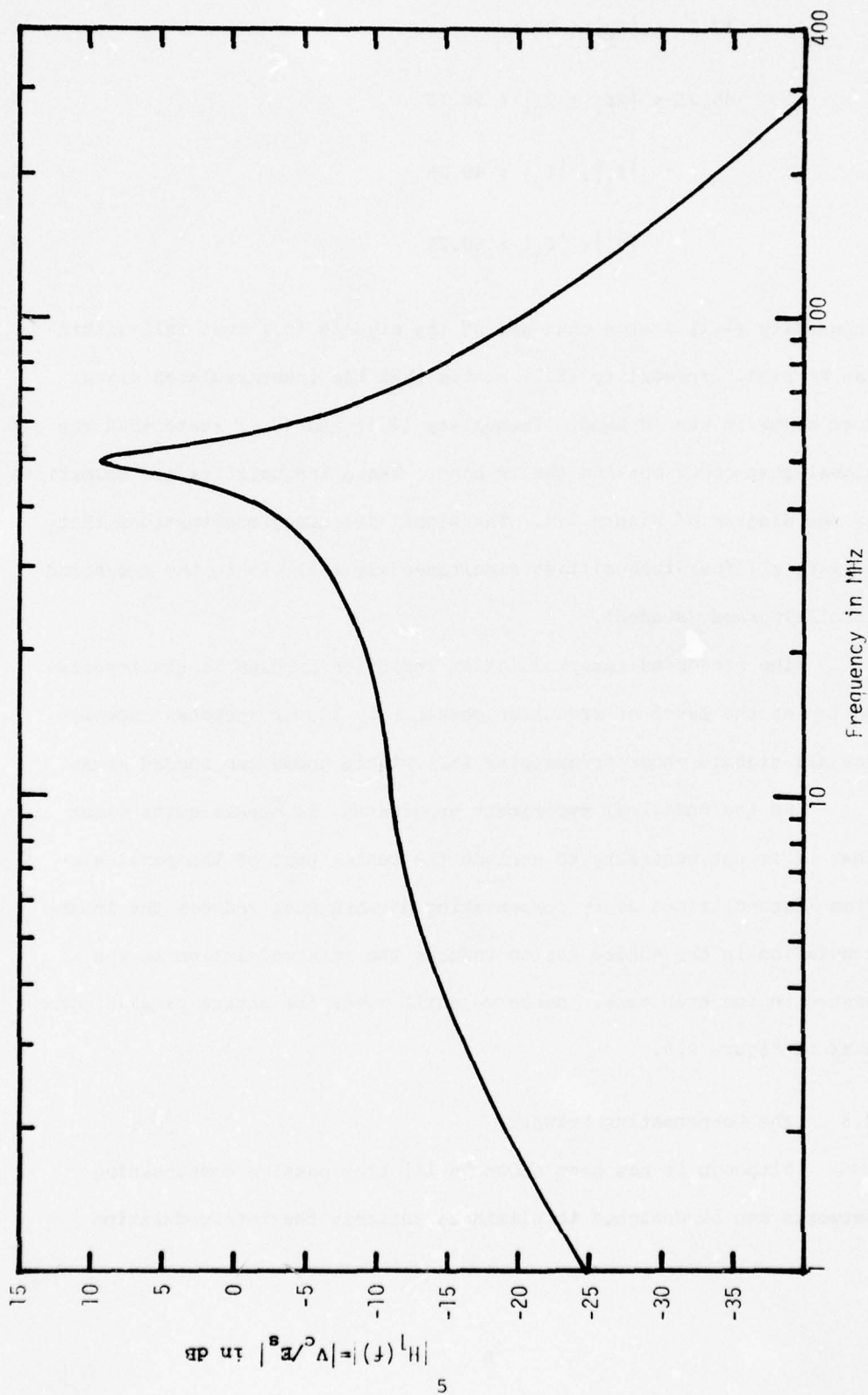


FIGURE 2.3. Linear Amplifier Response Without Compensation

$$47.5 < |f_1| < 52.5 \quad (2.1)$$

$$49.25 < |2f_1 + f_2| < 50.75 \quad (2.2)$$

$$|f_1|, |f_2| < 49.25 \quad (2.3)$$

$$|f_1|, |f_2| > 50.75 \quad (2.4)$$

Inequality (2.1) states that one of the signals ( $f_1$ ) must fall within the RF band. Inequality (2.2) states that the intermodulated signal must occur in the IF band. Inequality (2.3) and (2.4) state that the signal must occur outside the IF band. These inequalities are summarized in the diagram of Figure 2.4. The signal frequency combinations that satisfy all four inequalities simultaneously fall within the two solid parallelograms (shaded).

The broadband intermodulation reduction problem is the investigation of the level of reduction possible by linear response redesign for all signals whose frequencies fall within these two shaded areas.

As the numerical experiment progressed, it became quite clear that it is not necessary to exclude the center part of the parallelogram (dashed) since every compensating network that reduces the intermodulation in the shaded region reduces the intermodulation in the dashed region even more. Hence we shall cover the entire parallelogram AKMX of Figure 2.4.

### 2.3 The Compensating Network

Although it has been shown in [1] that passive compensating networks can be designed to eliminate entirely the intermodulation

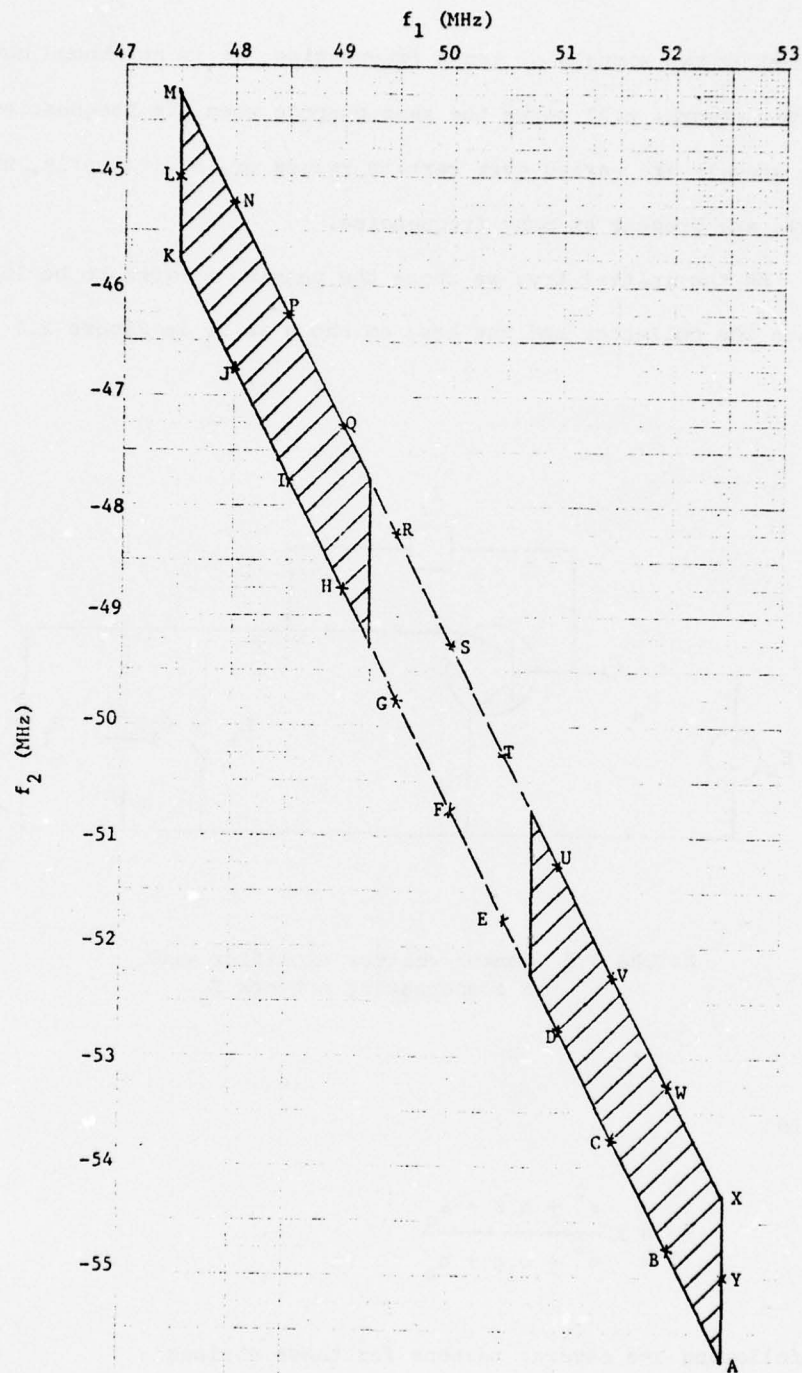


Fig. 2.4. Frequency combinations that produce third-order intermodulation in the IF band.



produced by two signals of known frequencies, it is not known how passive networks will serve the same purpose when the frequencies of these signals are varied over certain ranges or, equivalently, when signals are present at many frequencies.

As the initial try, we chose the passive network to be located between the collector and the base as shown as  $Y_3$  in Figure 2.5

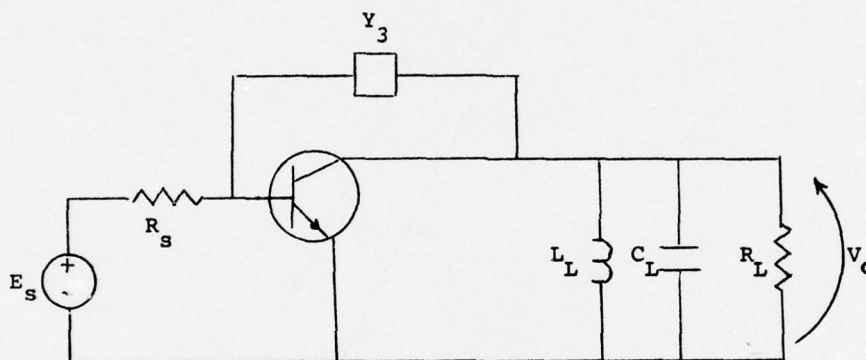


FIGURE 2.5 Common-emitter amplifier with a compensating network  $Y_3$ .

and let

$$Y_3 = K \frac{s^2 + a_1 s + a_0}{s^2 + b_1 s + b_0} \quad (2.5)$$

The following are several reasons for these choices:

- (1) This position for  $Y_3$  was found to be most effective from the previous study.

- (2) The realizability condition and synthesis techniques for the admittance of (2.5) is well known and it includes numerous simpler circuits as special cases of this admittance.
- (3) There are five coefficients in the expression of (2.5) available as parameters for optimization. This should offer a good versatility and at the same time not make the computation too complex.
- (4) The network for  $Y_3$  is of reasonable complexity and yet offers some flexibility in its characteristic.

It is further assumed, ideally, that  $Y_3 = 0$  for frequencies in the pass band of the amplifier. This is necessary so the linear response of the amplifier in the pass band will not be disturbed.

#### 2.4 Relationship in the Equivalent Circuit of the Amplifier

The equivalent circuit of the amplifier of Figure 2.5 is shown in Figure 2.6 in which the source has been replaced by its Norton's equivalent. Using the node designation as shown in Figure 2.6, the admittance matrix is

$$[Y(s)] = \begin{bmatrix} g_s + sC_1 + g_b + sC_3 + Y_3 & -g_b & -sC_3 - Y_3 \\ -g_b & g_b + k_1 + sC_2 + g_c - \alpha k_1 & -g_c \\ -sC_3 - Y_3 & -g_c + \alpha k_1 & g_c + g_L + sC_3 + sC_L + \frac{1}{sL_L} + Y_3 \end{bmatrix} \quad (2.6)$$

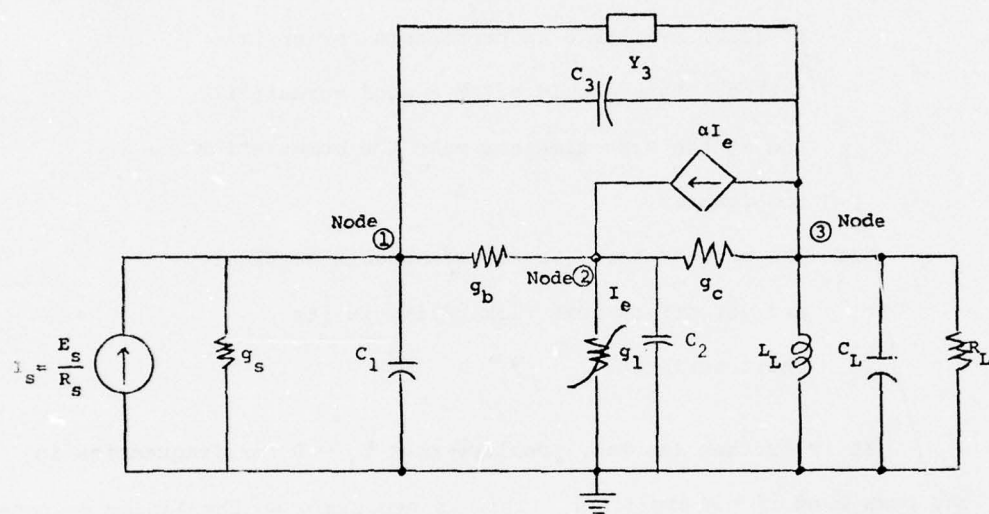


FIGURE 2.6. Equivalent Circuit of the Common-Emitter Amplifier of Figure 2.5.

As was derived in [1], if  $[Y]$  is unchanged in the pass band, then the third-order intermodulation is proportional to

$$P = (\alpha-1)[Z_{22}(2f_1) + 2Z_{22}(f_1+f_2)] - \alpha[Z_{23}(2f_1) + 2Z_{23}(f_1+f_2)] + \frac{3g_3}{2g_2^2} \quad (2.7)$$

where:

$$\begin{bmatrix} Z_{11} & Z_{12} & Z_{13} \\ Z_{21} & Z_{22} & Z_{23} \\ Z_{31} & Z_{32} & Z_{33} \end{bmatrix} = [Y]^{-1} \quad (2.8)$$

The quantity  $|P|^2$ , with  $P$  given in (2.7), is the cost function that is to be minimized according to the various criteria established for the study.

## 2.5 The Optimization Program

The algorithm used in this experiment to minimize the third-order intermodulation uses a modified Fletcher-Powell method. The algorithm was originally developed for another Post-Doctoral Program task [4]. It is a constrained minimization algorithm modified to minimize the cost function  $|P|^2$  with  $P$  given in (2.7) and  $Y_3$  given in (2.5). The constraints are

$$\begin{aligned} a_1 &\geq 0 & b_0 &\geq 0 \\ a_0 &\geq 0 & K &\geq 0 \\ b_1 &\geq 0 \end{aligned} \quad (2.9)$$



and

$$a_1 b_1 \geq (\sqrt{a_0} - \sqrt{b_0})^2 \quad (2.10)$$

Constraint (2.10) is the condition under which  $Y_3$  will be positive-real [5] and, therefore, realizable.

## 2.6 Third-Order Intermodulation of the Amplifier

For convenience, a series of points along the sides of the parallelogram of combinations of  $f_1$  and  $f_2$  of Figure 2.4 are chosen. Effort is then expended to reduce the third-order intermodulation along these sides. It is presumed, and later verified, that when intermodulation is reduced along the border of the parallelogram, the intermodulation is reduced by a larger amount in the interior of the parallelogram. Hence, we only need be concerned with the performance of the compensating network along this border. The point designation of these points is given in Figure 2.4 and their corresponding frequency combinations tabulated in Table 2.1. Table 2.1 also gives the third-order transfer function  $H_3(f_1, f_1, f_2)$  of the original amplifier without the compensation network. It is this function that we are striving to reduce in this study.

## 2.7 Maximum Average Reduction at the Four Vertexes of the Parallelogram

The first criterion used in the optimization algorithm is to reduce the average third-order intermodulation at the four vertexes of the parallelogram of Figure 2.4. The constrained optimization algorithm is applied to the five variables of  $Y_3$  of (2.5) such that the sum of the cost function  $|p|^2$  at the four points, A, K, M, and X of

TABLE 2.1  
 FREQUENCY COMBINATION AND THIRD-ORDER  
 INTERMODULATION OF THE TRANSISTOR AMPLIFIER

POINT	$f_1$ (MHz)	$f_2$ (MHz)	$2f_1 + f_2$ (MHz)	$H_3(f_1, f_1, f_2)$ (V/V <sup>3</sup> )
A	52.5	-55.75	49.25	0.38705 /-17.30°
B	52.0	-54.75	49.25	0.34568 /-17.53°
C	51.5	-53.75	49.25	0.28230 /-19.87°
D	51.0	-52.75	49.25	0.20143 /-27.07°
E	50.5	-51.75	49.25	0.12039 /-44.38°
F	50.0	-50.75	49.25	0.06460 /-74.54°
G	49.5	-49.75	49.25	0.05253 /-89.26°
H	49.0	-48.75	49.25	0.11495 /-92.68°
I	48.5	-47.75	49.25	0.24147 /-103.59°
J	48.0	-46.75	49.25	0.39108 /-110.52°
K	47.5	-45.75	49.25	0.53420 /-113.92°
L	47.5	-45.00	50.00	0.55480 /-137.47°
M	47.5	-44.25	50.75	0.51888 /-159.13°
N	48.0	-45.25	50.75	0.40178 /-157.82°
P	48.5	-46.25	50.75	0.27691 /-152.42°
Q	49.0	-47.25	50.75	0.16379 /-137.80°
R	49.5	-48.25	50.75	0.08718 /-107.14°
S	50.0	-49.25	50.75	0.05469 /-73.83°
T	50.5	-50.25	50.75	0.07258 /-77.33°
U	51.0	-51.25	50.75	0.15714 /-75.11°
V	51.5	-52.25	50.75	0.26063 /-68.35°
W	52.0	-53.25	50.75	0.34729 /-64.06°
X	52.5	-54.25	50.75	0.40674 /-61.78°
Y	52.5	-55.0	50.00	0.41753 /-39.38°

Figure 2.4 is minimum. The optimization scheme gives

$$\begin{aligned}
 K &= 0.054428 \\
 a_1 &= 286.75 \times 10^7 \\
 a_0 &= 146.157 \times 10^{14} \\
 b_1 &= 4.23085 \times 10^7 \\
 b_0 &= 127.046 \times 10^{14}
 \end{aligned} \tag{2.11}$$

The network to furnish an  $Y_3$  with these coefficients is obtained by Foster's Preamble [6] and is given in Figure 2.7.

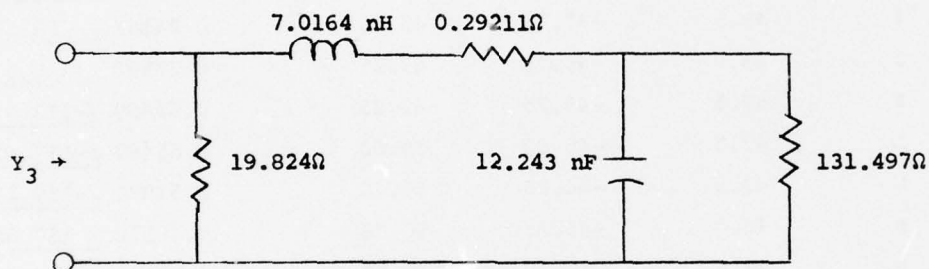


FIGURE 2.7. Network to Give the Admittance of (2.5) with Coefficients Given in (2.11).

The amount of reduction along the border of the parallelogram obtained from this compensating network is tabulated in Table 2.2. If we take the ratio of the sums of the cost function  $|P|^2$  at the four vertexes without  $Y_3$  and those with the optimum  $Y_3$ , it is equal to 15.73 which corresponds to an average reduction of 11.97 dB. The relative value of  $|H_3|$  along the parallelogram is shown in Figure 2.8.

TABLE 2.2  
RELATIVE COST FUNCTIONS OBTAINED BY  
MAXIMIZING THE AVERAGE REDUCTION AT THE FOUR VERTEXES \*

POINT	COST FUNCTION $ P ^2$ WITHOUT $Y_3$	COST FUNCTION $ P ^2$ WITH $Y_3$ COEFFICIENTS OF (2.11)	THIRD-ORDER INTERMODULA- TION REDUCTION dB
A*	0.22064	0.03241	8.39
B	0.23723	0.023939	9.96
C	0.25367	0.016911	11.76
D	0.26907	0.012145	13.46
E	0.28238	0.010407	14.34
F	0.29247	0.011297	14.13
G	0.29841	0.011555	14.12
H	0.29960	0.007645	15.93
I	0.29599	0.003011	19.93
J	0.28804	0.002330	20.92
K*	0.27661	0.005774	16.80
L	0.25507	0.003859	18.20
M*	0.23146	0.002290	20.05
N	0.24715	0.000628	25.95
P	0.26240	0.000083	35.02
Q	0.27630	0.000805	25.36
R	0.28778	0.004071	18.50
S	0.29578	0.011620	14.06
T	0.29944	0.02205	11.33
U	0.29830	0.02749	10.36
V	0.29241	0.025130	10.66
W	0.28236	0.022145	11.06
X*	0.26909	0.023045	10.67
Y	0.24554	0.025789	9.79

\* Vertexes of the frequency parallelogram of Figure 2.4.



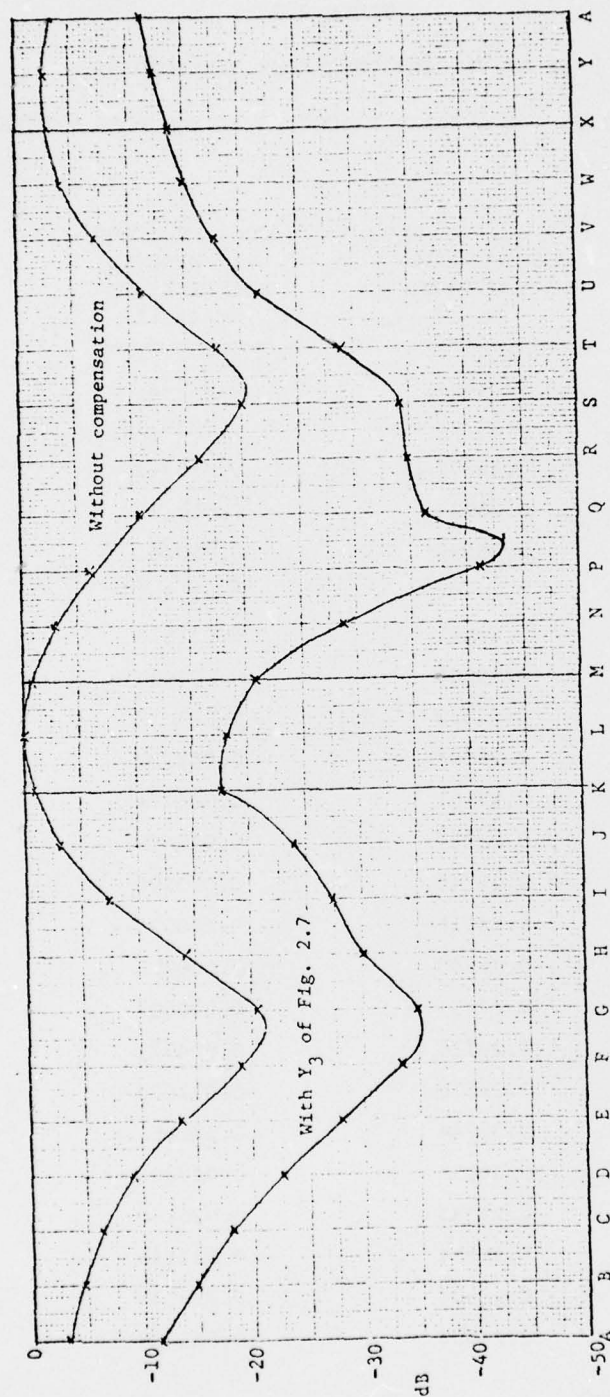


Fig. 2.8. Relative third-order transfer functions along the border of the frequency parallelogram when the average reduction at the vertexes is maximized.

Under this criterion, the average reduction in the frequency band of interest is obtained by selecting a larger number of points throughout the parallelogram and then summing up the cost functions at these points. The approximate reduction is then obtained by comparing this sum to the sum of the cost functions when  $Y_3$  is absent. This approximate reduction is found to be 13.51 dB.

#### 2.8 Maximum Average Reduction Along the Border

The second criterion used is to maximize the average reduction along the border of the parallelogram. This is done by minimizing the sum of the cost functions at the 24 points, A-Y, chosen along the border as indicated in Figure 2.4. The resulting optimum network function coefficients are

$$\begin{aligned} K &= 0.05 \\ a_1 &= 340 \times 10^7 \\ a_0 &= 100 \times 10^{14} \\ b_1 &= 0.1 \times 10^7 \\ b_0 &= 120 \times 10^{14} \end{aligned} \quad (2.12)$$

The network that gives these coefficients is shown in Figure 2.9.

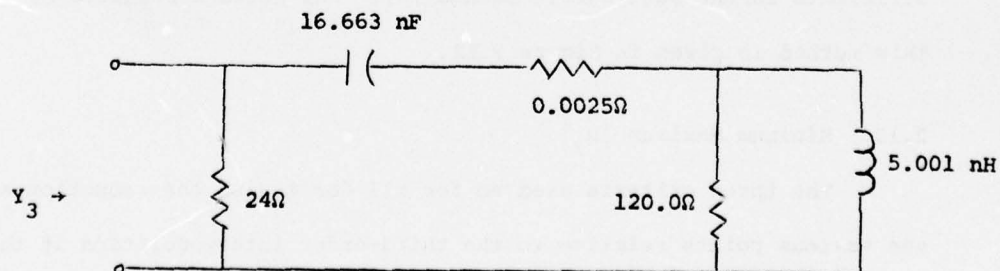


FIGURE 2.9. Network To Give  $Y_3$  of (2.5) With Coefficients Given in (2.12).

The distribution of the reduction of third-order intermodulation is tabulated in Table 2.3 and plotted in Figure 2.10. For this criterion, the average reduction is approximately 14.13 dB along the border.

## 2.9 Maximum-Minimum Reduction Along the Border

The third criterion chosen is to find the coefficients of  $Y_3$  of (2.5) such that the minimum reduction along the border of the frequency parallelogram is maximum. These coefficients are found to be:

$$\begin{aligned} K &= 0.05 \\ a_1 &= 360 \times 10^7 \\ a_0 &= 100 \times 10^{14} \\ b_1 &= 0.1 \times 10^7 \\ b_0 &= 195 \times 10^{14} \end{aligned} \tag{2.13}$$

The distribution of the reduction along the border is tabulated in Table 2.4 and plotted in Figure 2.11. Under this criterion, the minimum reduction of 9.73 dB occurs at point K. The average reduction throughout the parallelogram is found to be approximately 12.97 dB.

To realize  $Y_3$  with coefficients given in (2.13), Foster's Preamble is no longer adequate. One method of realizing these coefficients is the Bott-Duffin method [6]. The network realized by this method is given in Figure 2.12.

## 2.10 Minimum Maximum $|H_3|$

The three criteria used so far all dealt with the reduction at the various points relative to the third-order intermodulation at those

TABLE 2.3  
RELATIVE COST FUNCTIONS OBTAINED BY  
MAXIMIZING THE AVERAGE REDUCTION ALONG THE BORDER

POINT	COST FUNCTION $ P ^2$ WITHOUT $Y_3$	COST FUNCTION $ P ^2$ WITH $Y_3$ COEFFICIENTS OF (2.12)	THIRD-ORDER INTERMODULA- TION REDUCTION dB
A	0.22064	0.027614	9.03
B	0.23723	0.019195	10.92
C	0.25367	0.011941	13.27
D	0.26907	0.006648	16.07
E	0.28238	0.004256	18.21
F	0.29247	0.005409	17.33
G	0.29841	0.008142	15.64
H	0.29960	0.007003	16.31
I	0.29599	0.006194	16.80
J	0.28804	0.010286	14.47
K	0.27661	0.018356	11.78
L	0.25507	0.012988	12.93
M	0.23146	0.008532	14.33
N	0.24715	0.003933	17.98
P	0.26240	0.001450	22.58
Q	0.27630	0.000397	28.43
R	0.28778	0.001540	22.72
S	0.29578	0.007515	15.95
T	0.29944	0.019607	11.83
U	0.29830	0.024406	10.87
V	0.29241	0.017577	12.21
W	0.28236	0.013858	13.09
X	0.26909	0.015944	12.27
Y	0.24554	0.020511	10.78



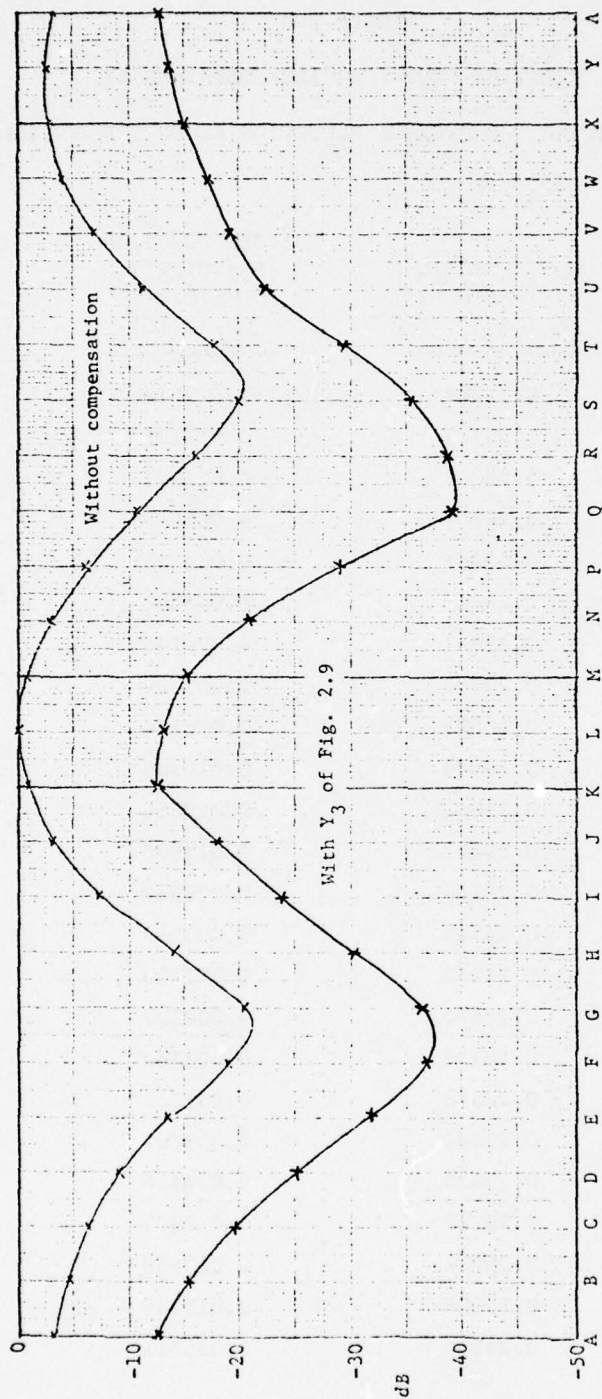


Fig. 2.10. Relative third-order transfer functions along the border of the frequency parallelogram when the average reduction along the border is maximized.

TABLE 2.4  
RELATIVE COST FUNCTIONS OBTAINED BY  
MAXIMIZING THE MINIMUM REDUCTION ALONG THE BORDER

POINT	COST FUNCTION $ P ^2$ WITHOUT $Y_3$	COST FUNCTION $ P ^2$ WITH $Y_3$ COEFFICIENTS OF (2.13)	THIRD-ORDER INTERMODULA- TION REDUCTION dB
A	0.22064	0.023016	9.82
B	0.23723	0.015194	11.94
C	0.25367	0.008892	14.55
D	0.26907	0.005004	17.31
E	0.28238	0.004459	18.02
F	0.29247	0.007504	15.91
G	0.29841	0.011794	14.03
H	0.29960	0.013312	13.52
I	0.29599	0.014645	13.06
J	0.28804	0.019908	11.60
K	0.27661	0.029411	9.73
L	0.25507	0.020925	10.86
M	0.23146	0.013915	12.21
N	0.24715	0.007924	14.94
P	0.26240	0.004743	17.43
Q	0.27630	0.003859	18.55
R	0.28778	0.006344	16.57
S	0.29578	0.014414	13.12
T	0.29944	0.026482	10.53
U	0.29830	0.029887	9.99
V	0.29241	0.021631	11.31
W	0.28236	0.014538	12.88
X	0.26909	0.013561	12.98
Y	0.24554	0.016147	11.82

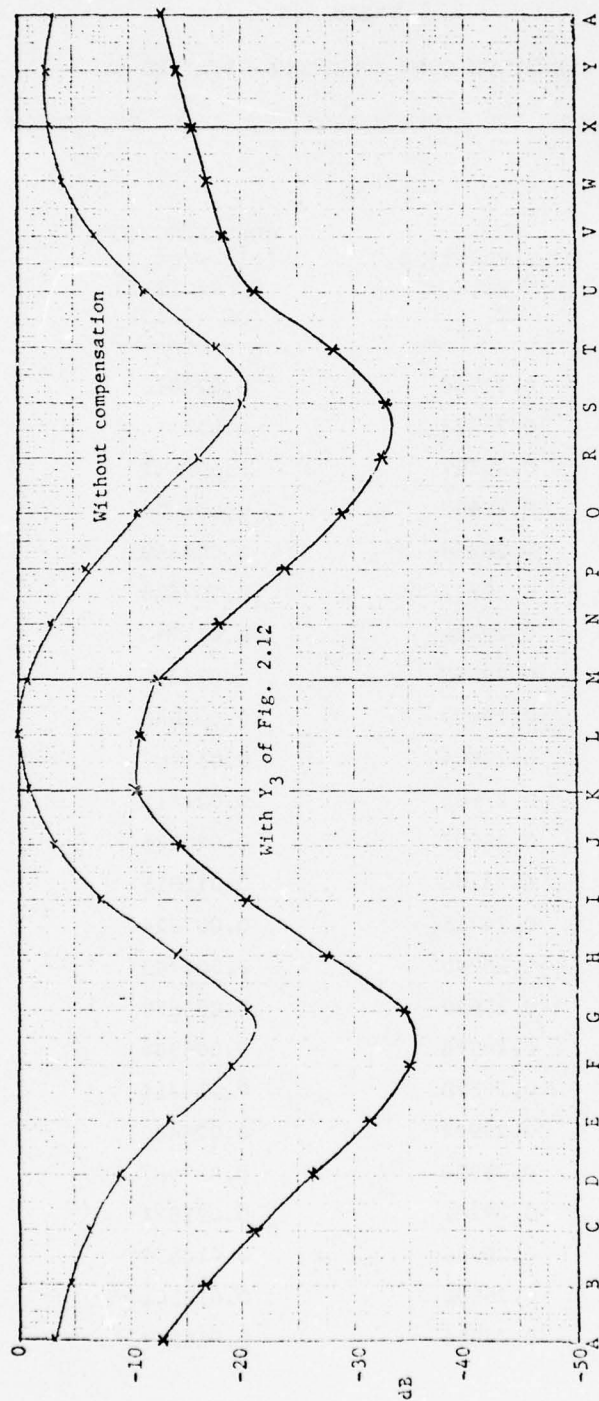


Fig. 2.11. Relative third-order transfer functions along the border of the frequency parallelogram when the minimum reduction along the border is maximized.

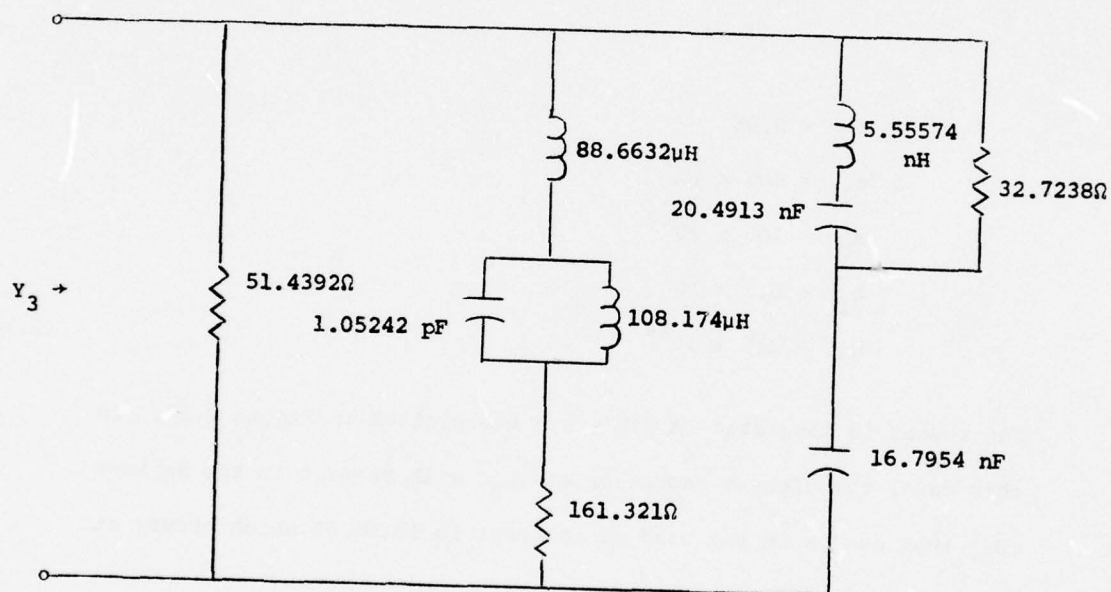


FIGURE 2.12. Network to Give  $Y_3$  of (2.5) With Coefficients Given in (2.13).



respective points. The fourth criterion used is to reduce the absolute value of  $|H_3|$  so that the maximum  $|H_3|$  after compensation is made minimum. In carrying out this computation, before comparing the relative cost functions, each reference cost function is preadjusted to reflect this difference. Thus, the same algorithm is used to obtain the network function coefficients until the maximum ratio of the cost functions with  $Y_3$  present and without  $Y_3$  is made minimum. The coefficients for  $Y_3$  to achieve this reduction are:

$$\begin{aligned} K &= 0.05 \\ a_1 &= 300 \times 10^7 \\ a_0 &= 100 \times 10^{14} \\ b_1 &= 0.2 \times 10^7 \\ b_0 &= 210 \times 10^{14} \end{aligned} \tag{2.14}$$

The result is tabulated in Table 2.5 and plotted in Figure 2.13. In this case, the highest reduction of  $|H_3|$  with respect to the maximum  $|H_3|$  that occurs in the band of interest is 13.06 dB which occurs at Point L.

To obtain the network for this  $Y_3$ , Bott-Duffin method will also have to be used. The network will be exactly like that of Figure 2.12 with the element values slightly altered.

#### 2.11 Addition of $Y_1$

The third-order intermodulation reduction rendered by  $Y_3$  above is rather modest when  $Y_3$  only is employed. In order to further

TABLE 2.5  
EQUIVALENT RELATIVE COST FUNCTIONS OBTAINED  
BY MINIMIZING THE MAXIMUM  $|H_3|$

POINT	EQUIVALENT COST FUNCTION P <sup>2</sup> WITHOUT Y <sub>3</sub>	COST FUNCTION P <sup>2</sup> WITH Y <sub>3</sub> COEFFICIENTS OF (2.14)	THIRD-ORDER INTERMODULA- TION REDUCTION dB
A	0.45333	0.022179	13.10
B	0.61106	0.014949	16.12
C	0.97977	0.010224	19.82
D	2.0413	0.009145	23.49
E	5.9967	0.012181	26.92
F	21.572	0.017275	30.96
G	33.282	0.018416	32.57
H	6.9788	0.012008	27.64
I	1.5625	0.005458	24.57
J	0.57969	0.006287	19.65
K	0.29835	0.014406	13.16
L	0.25507	0.012623	13.06
M	0.26462	0.009798	14.32
N	0.47126	0.004591	20.11
P	1.0533	0.001317	29.03
Q	3.1699	0.000530	37.76
R	11.654	0.004477	34.16
S	30.434	0.015743	32.86
T	17.494	0.031568	27.44
U	3.7185	0.039710	19.72
V	1.3250	0.034309	15.87
W	0.72061	0.024807	14.63
X	0.50064	0.019561	14.08
Y	0.43353	0.017197	14.02

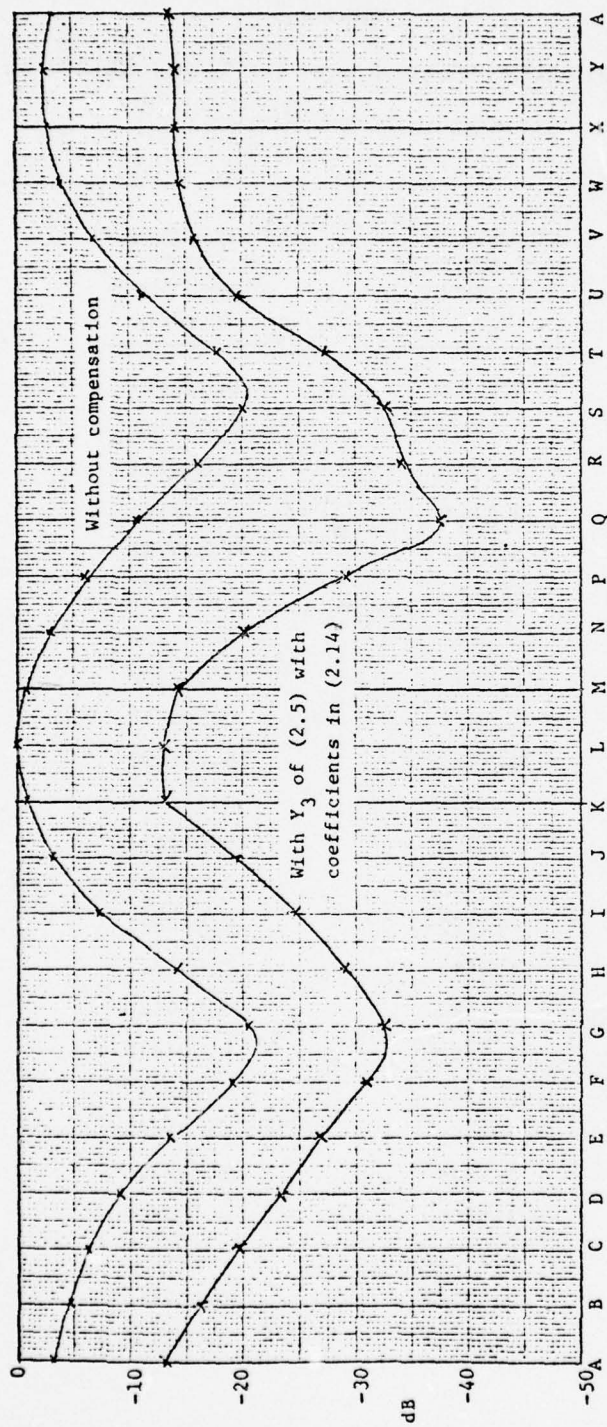


Fig. 2.13. Relative third-order transfer functions along the border of the frequency parallelogram when the maximum of  $|H_3|$  along the border is minimized.

enhance this reduction, several other schemes were tried. The first of these is to employ an additional admittance  $Y_1$  as shown in Figure 2.14. The analytical form of  $Y_1$  is assumed a priori to be identical to the  $Y_3$  of (2.5). It is also assumed that  $Y_1 = 0$  for frequencies inside the pass band. Thus, there are ten variables available for optimization. The same modified Fletcher-Powell optimization algorithm is again employed to find the variables to give the highest reduction under various criteria.

It was found under each of the criteria used, the addition of  $Y_1$  only gives a very slight improvement in the reduction of intermodulation. The additional reduction is in the order of 1 to 2 dB. From practical point of view, this reduction is insignificant.

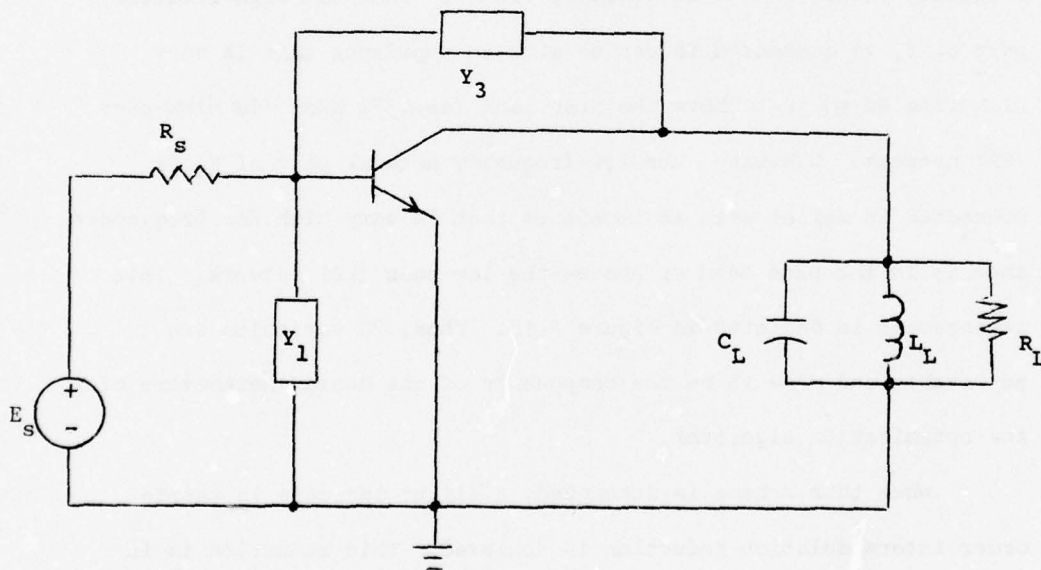


FIGURE 2.14. Amplifier With Two Compensating Networks,  $Y_1$  and  $Y_3$ .



## 2.12 Two Separate Networks for High-Frequency and Low-Frequency Compensation

Since the third-order intermodulation is a function of the second-order intermodulation and since the latter has frequencies at  $2f_1$  and  $f_1+f_2$ , the compensation of our scheme takes place at both high-frequencies,  $2f_1$ , and low-frequencies,  $f_1+f_2$ . If the compensating networks are allowed to be adjusted independently in these two ranges, it is possible that wide-band reduction of the third-order intermodulation can be increased over the case when the same compensating network must serve both frequency ranges.

In the second scheme in our attempt to increase the nonlinearity reduction, each network,  $Y_1$  or  $Y_3$ , is assumed to be made up of two independent subnetworks, each is only effective in either the high-frequency range or the low-frequency range. Thus the high-frequency part of  $Y_3$  is connected in series with an impedance that is very high from dc to just above the pass band (say, 70 MHz)--the high-pass (HP) network. Likewise, the low-frequency network part of  $Y_3$  is connected in series with an impedance that is very high for frequencies that is in the pass band or above--the low-pass (LP) network. This arrangement is depicted in Figure 2.15. Thus, 20 variables are adjustable and made to be the components of the design parameters of the optimization algorithm.

When this scheme is attempted, a slight increase in third-order intermodulation reduction is achieved. This reduction is in the order of 4 to 5 dB. This additional reduction is again judged to be very small considering the additional physical components required to implement these compensating networks.

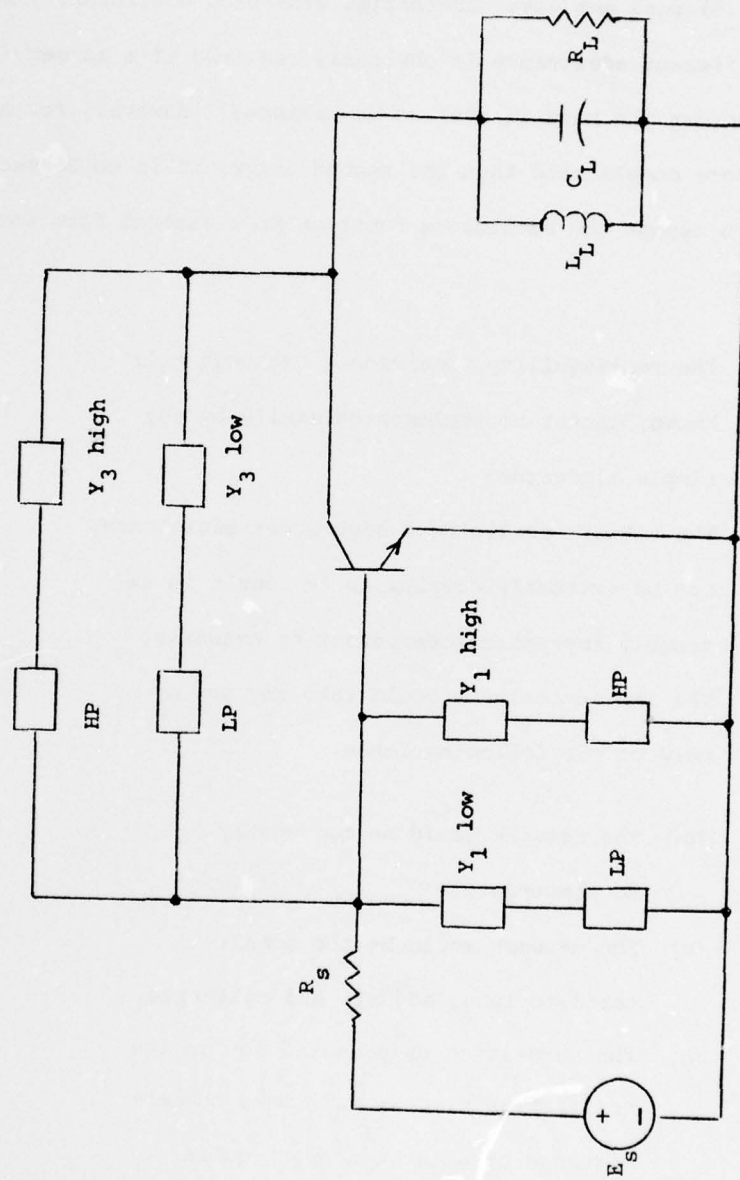


FIGURE 2.15. Amplifier With Four Compensating Networks.

### 2.13 The Search for an Idealized Compensating Network

At this point, it is quite clear that the assumed admittance function (2.5) does not give substantial wide-band nonlinearity reduction. A different admittance is obviously required if a larger reduction across the band is ever to be achieved. However, for admittances more complicated than the second order, it is no longer practical to assume the admittance function in a general form for two reasons:

- (1) The realizability conditions, although well known, cannot be implemented easily by any simple algorithm.
- (2) The network realizing a high-order admittance, can be extremely complex as to result in extremely impractical compensating networks. The impracticalness could take any one or more of the following forms:
  - (a) The network would be too costly to construct.
  - (b) The network would be too complicated to tune, adjust, and calibrate.
  - (c) The parasitics unaccounted for in the realization process will make the admittance of a large network quite different from the computed admittance.

There appears to be two re-courses to find more complex compensating networks to achieve further reduction. One of these is to assume specific networks a priori. In doing this, the only constraints we have would be that all element values be positive. The other alternative would be to search for the required admittance values point-by-point throughout the band. We know from previous studies that this is possible. Once this is known, we can then try to approximate these admittance values by a finite passive network. Since this second scheme appears to be more promising and the procedure is more concrete, we have adopted this scheme.

After considerable computational effort, it was found that the desired admittances should have the variations shown as solid curves in Figure 2.16. These admittances will enable us to achieve an across-the-band reduction of 40 dB or more which would be considered very satisfactory.

Two of these four admittances can be approximated by fairly simple networks. The circuit of Figure 2.17 (a) is designed to have exactly the values given in Figure 2.16 (a) at the two end points-- 95 MHz and 105 MHz. The shapes of the admittance curves of this circuit are almost straight lines in this range. These curves are shown as dashed curves in Figure 2.16 (a). Other approximation criteria can be applied to give other forms of approximation if desired.

The admittance of Figure 2.16(d) may be approximated by a simple RC parallel combination as shown in Figure 2.17 (b). The admittance of this circuit is shown in Figure 2.16(d) as dashed curves.



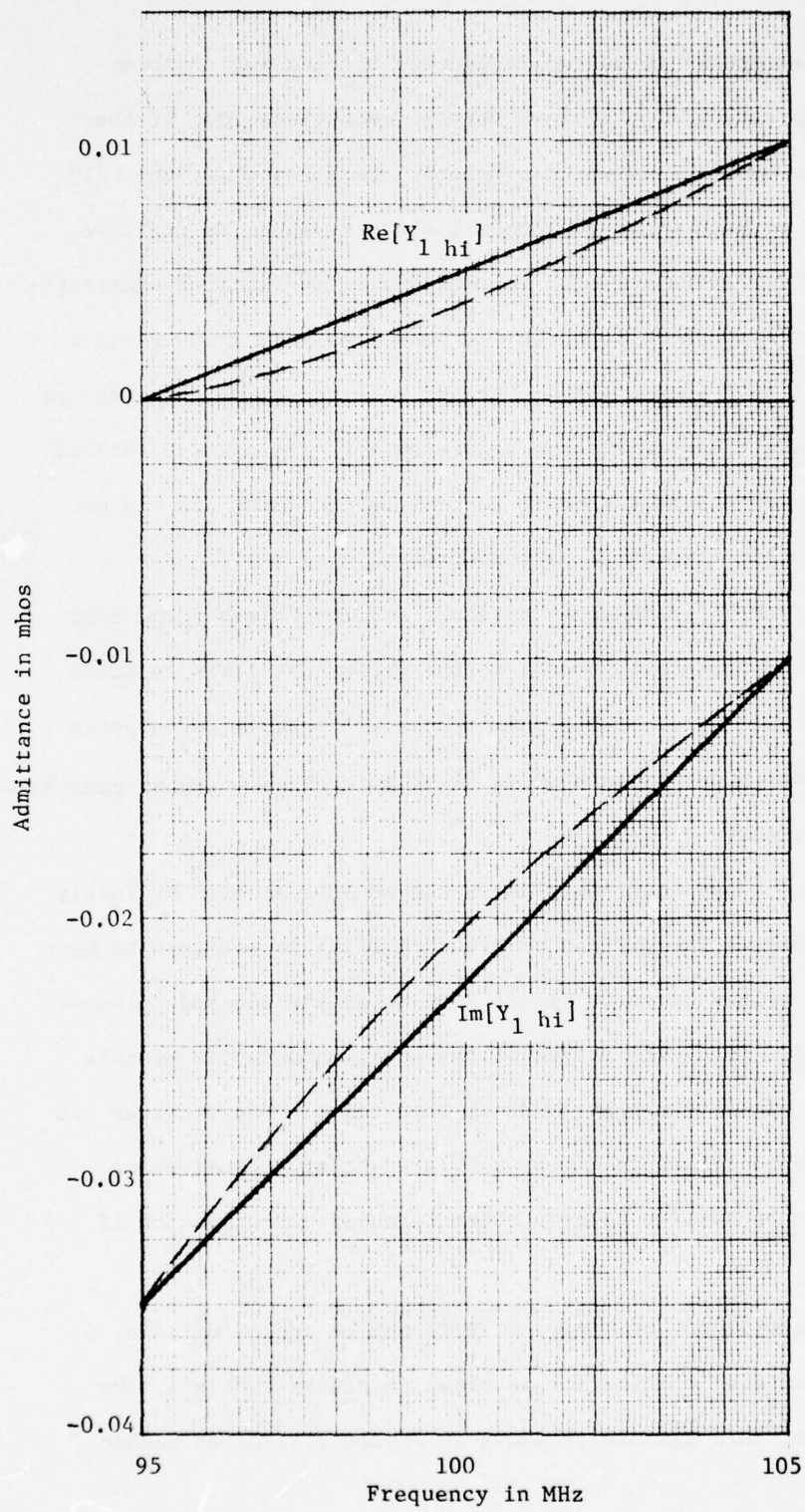


Fig. 2.16 (a). Ideal (solid) and approximate (dashed)  $Y_{1 \text{ hi}}$ .

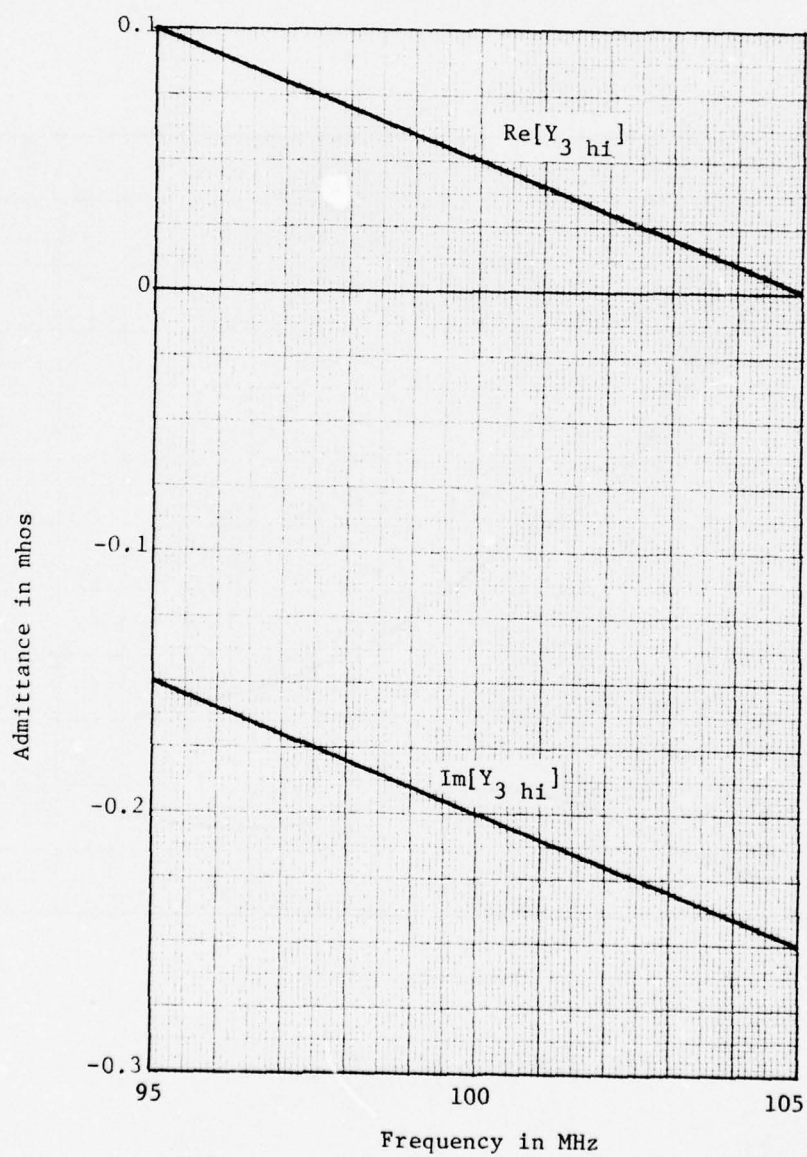


Fig. 2.16 (b). Ideal  $Y_{3\ hi}$ .

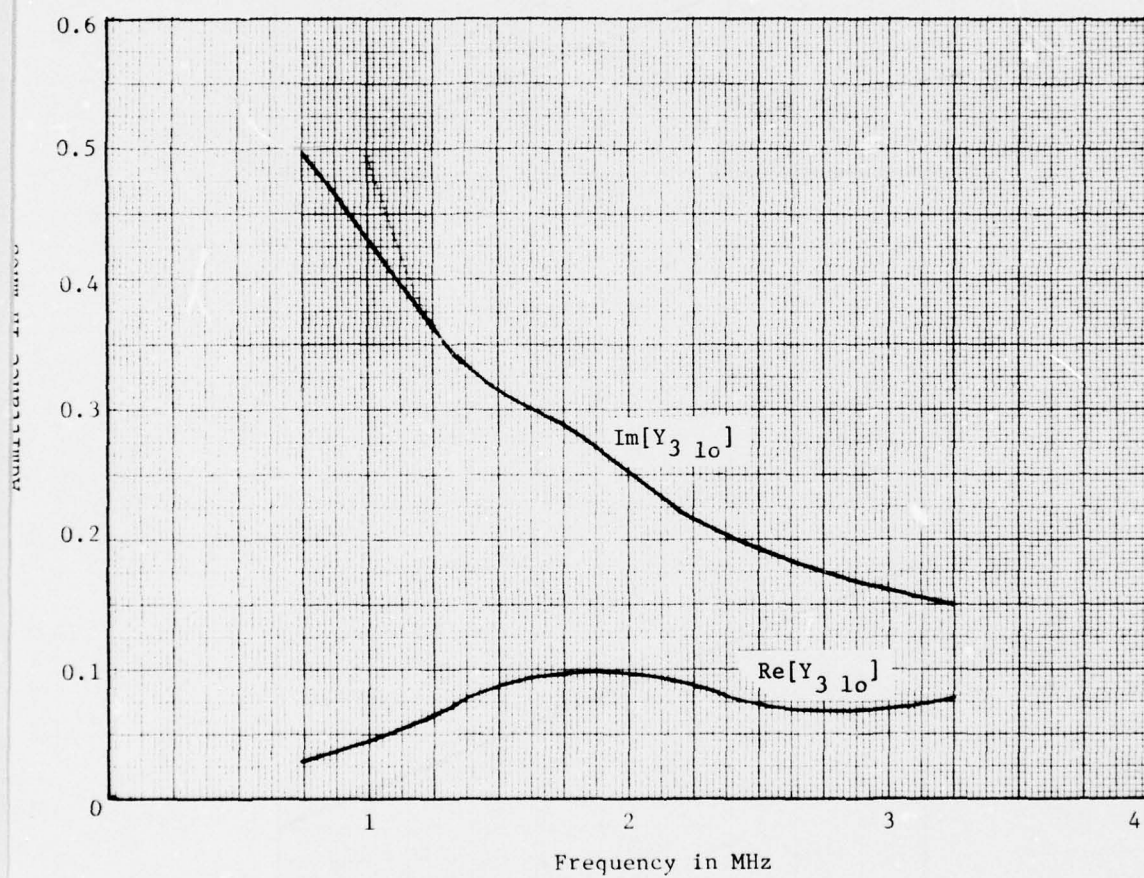


Fig. 2.16(c). Ideal  $Y_{1 10}$ .



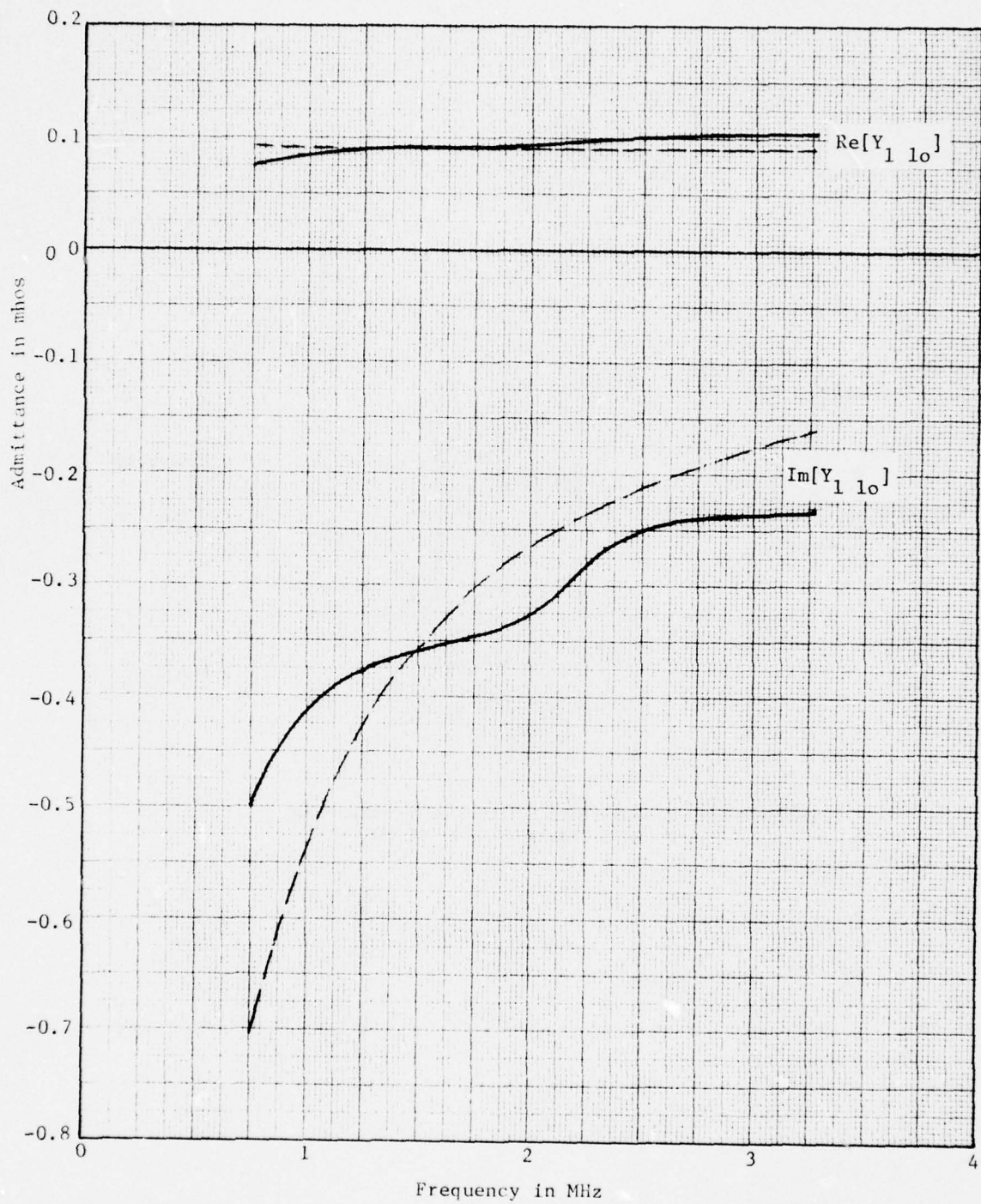


Fig. 2.16(d). Ideal (solid) and approximate (dashed)  $Y_{110}$ .



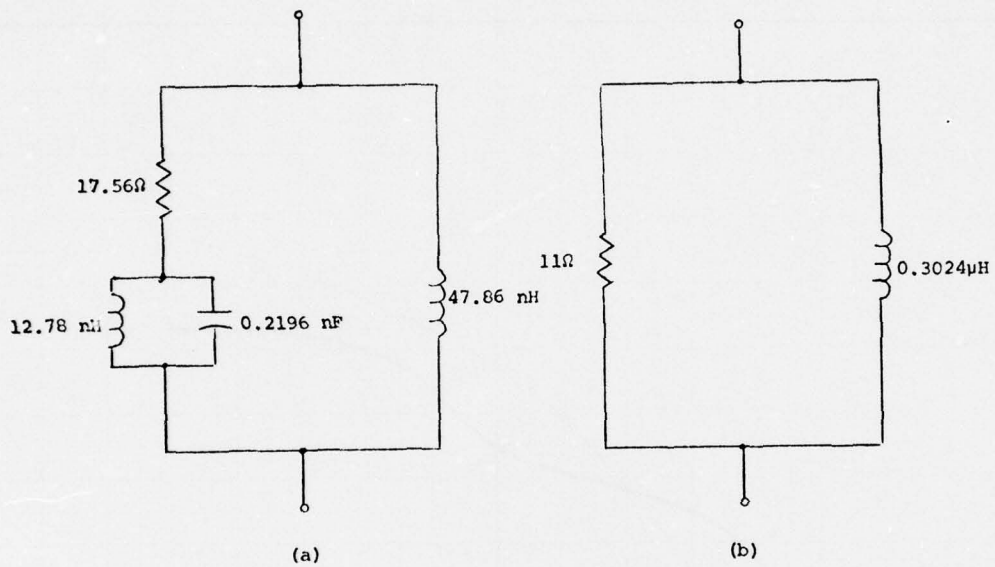


FIGURE 2.17. Networks With Admittances Approximating Those of Figure 2.16(a) and (d).

The two admittances shown in Figure 2.16(b) and (c), which are necessary to produce the satisfactory level of reduction, is very difficult, if not impossible, to realize. Numerous methods have been tried and only very poor approximations have been obtained. These poor approximations give inferior performance to the broad-band nonlinearity reduction produced by using the assumed admittance of (2.5) for all four impedances,  $Y_{1\ hi}$ ,  $Y_{1\ lo}$ ,  $Y_{3\ hi}$ , and  $Y_{3\ lo}$ .

#### 2.14 Conclusions and Conjectures

The numerical experimentation summarized in this Chapter was carried out to obtain an indication of how effective the passive compensation scheme that was successfully done for a single frequency combination, can be extended to a combination of ranges of frequency. Several tentative conclusions have been drawn from the result of this experiment.

One of the most important conjectures that is part of the conclusion of this experiment is that the complexity of the passive compensating network does not contribute to the reduction of third-order intermodulation. In many cases, the addition of new network elements assume extreme values thus reverting the assumed network to the simpler configuration that was in place originally. Although this conclusion has not been analytically and conclusively proved, the evidence is highly suggestive of this conjecture. Since this conjecture would be extremely difficult to prove analytically and since it would not be very beneficial even if this proof has been done, it was decided to let this conjecture stand on the basis that numerical experimental evidence tends to support it.

One of the reasons that could explain why most of the required wide-band  $Y_1$  and  $Y_3$  are not all realizable is that in compensating the third-order intermodulation at  $2f_1+f_2$ , we are attempting to redesign the amplifier circuit in frequency ranges that cover  $2f_1$  and  $f_1+f_2$ . In both of these two ranges, we are attempting to nullify the second-order responses. The second-order terms are typically the products or squares of first-order responses. Hence, we need to produce driving-point admittances that are the products or squares of passive driving-point or transfer functions. This is usually difficult to accomplish except for very narrow band applications. In our example,  $2f_1$  ranges from 95 to 105 MHz and can be considered a narrow-band realization. However,  $f_1+f_2$  ranges from 0.75 to 3.25 MHz which is over two octaves wide and cannot be regarded as a narrow-band situation. This seems to have led to the non-realizability of  $Y_1$  and  $Y_3$  in this range in Section 2.13.

Another conclusion that we have arrived at in the numerical experiment in the wide-banding effort concerns the use of the optimization algorithm. Although the algorithm developed in [1] and adopted for our current project worked well in arriving at the local minimum very rapidly and accurately, much of its success depends on the location of the starting point. In most of the effort in this chapter, frequently more effort was expended in searching for a reasonable starting point than to arrive at the accurate local minimum. For practical purposes, if the approximate valid starting point is known, the problem is almost solved. The optimization algorithm frequently only gives an improvement in the design vector elements

in the second or third significant figures.

In the course of the research of this chapter, as we progressed in our work, the computational effort gradually shifted from automatic optimization technique to systematic search routines. The latter simply involves a large amount of repetitive computation of certain cost function and the latter is gradually reduced by a combination of automatic search and man-machine interactive algorithm. This mode of computation is used almost exclusively in the effort that is to follow.



## CHAPTER III

### MEDIUM TO NARROW BAND INTERMODULATION REDUCTION

#### WITH EMITTER RESISTANCE NONLINEARITY ONLY

##### 3.1 Introduction

Based on the result obtained in Chapter II, it was observed that the technique of using passive compensating network to reduce third-order intermodulation was not particularly suited for wide-band applications. Since we are dealing with compensating networks that are themselves frequency sensitive, it should not be surprising that unless the required frequency behavior of the networks agree with the required frequency variation, the compensation is not likely to be effective over the frequency range in question. This fact was borne out in the search for the wide-band compensating network in Chapter II.

We shall now turn our attention to medium- and narrow-band applications. One purpose of this investigation is to ascertain, for a particular assumed amplifier, what is the bandwidth within which the passive compensating network would be effective. Another purpose is to determine the trade-off between bandwidth and the third-order intermodulation reduction.

##### 3.2 The Frequency Specification

The same amplifier used in Chapter II will again be used in this chapter. However, since the frequency range assigned in Chapter II turned out to be too ambitious, several modifications are made in this study.

First, the two signals that join to produce the third-order intermodulation must both fall within the RF band. In other words, in addition to (2.1) we further require that

$$47.5 < |f_2| < 52.5 \quad (3.1)$$

The tripling effect of the IF bandwidth is removed. In other words, inequality (2.2) is replaced by

$$49.75 < |2f_1 + f_2| < 50.25 \quad (3.2)$$

The new frequency region of interest, as compared to that considered in Chapter II, is depicted in Figure 3.1.

In addition to the reduction in bandwidth, the compensation network employed in this study will be as simple as possible. In all cases, the low-frequency admittance ( $Y_{1 \ 10}$  and  $Y_{3 \ 10}$ ) will always be a simple conductance. The high-frequency admittance will be that of an RL or an RC parallel combination. There are two reasons for this choice. One of them is that our experience gained in Chapter II indicates that the complexity of the passive network contributes little to the reduction of nonlinear effects. The other is that since we are primarily dealing with narrow-band phenomena here, the admittances need not vary to any great extent to produce adequate compensation.

### 3.3. Bandwidth and Reduction Trade-off

As a first investigation here, the bandwidth of  $|f_1|$  and  $|f_2|$  are altered. For each chosen bandwidth a search is made to find the optimum network parameters. The resultant reduction is then tabulated.

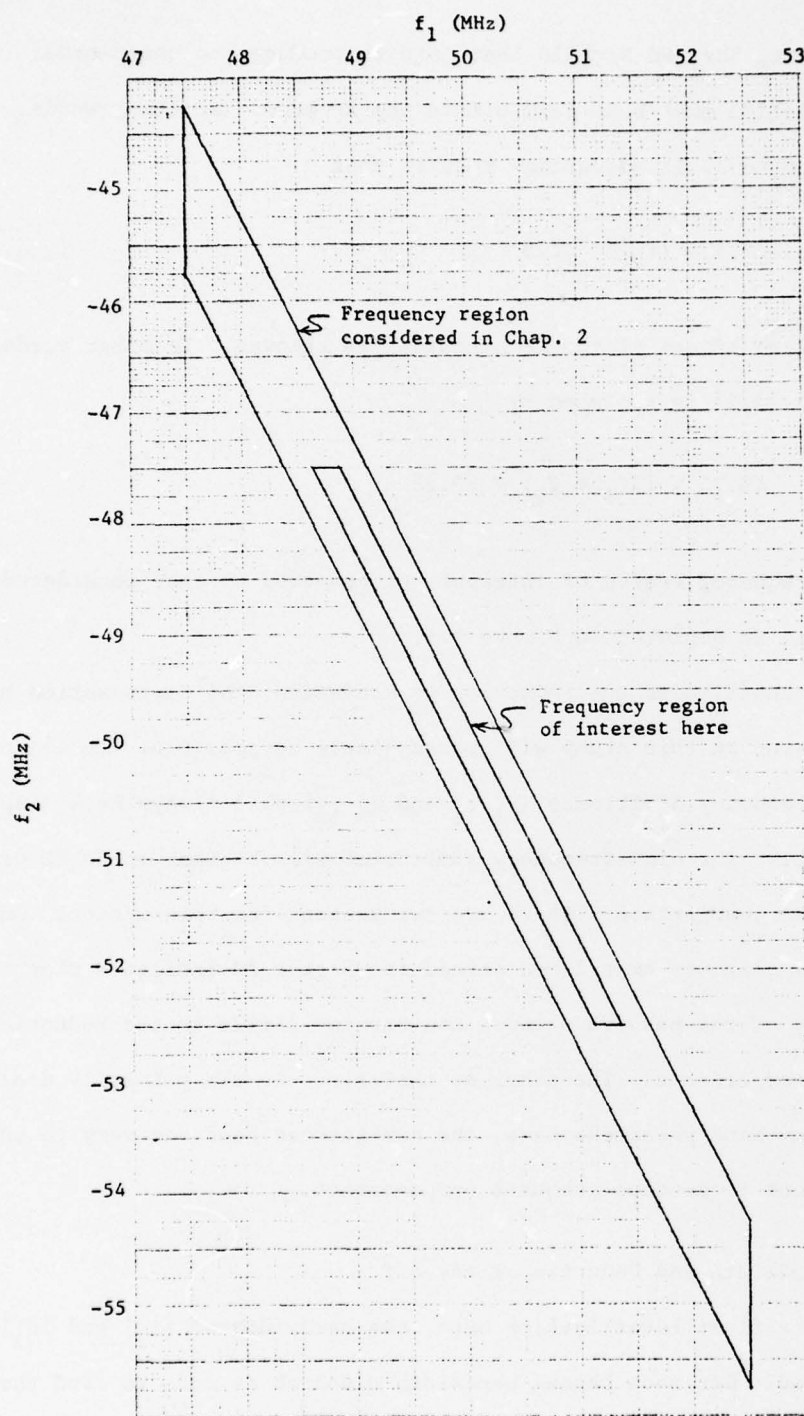


Fig. 3.1. Frequency regions of interest.

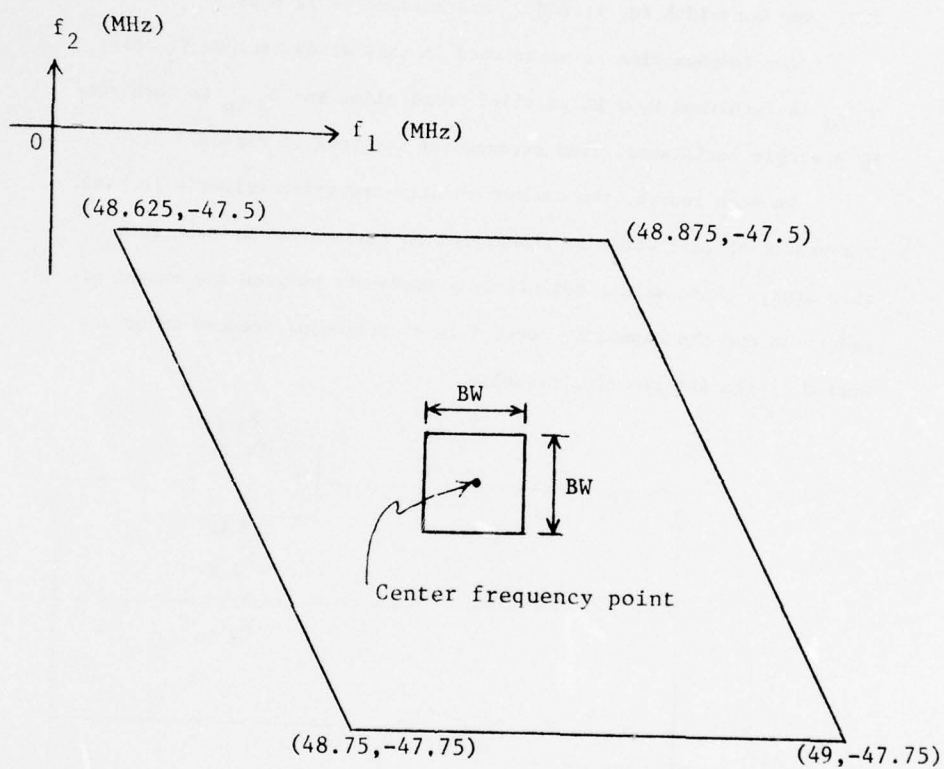


Fig. 3.2. Frequency regions used in the study of bandwidth and reduction trade-off.



The frequency ranges for  $f_1$  and  $f_2$  are chosen to be centered at  $f_1 = 48.8125$  and  $f_2 = -47.625$ . This is also the center of that part of the parallelogram of Figure 3.1 that lies between  $f_2 = -47.5$  and  $f_2 = -47.75$ . That part is another parallelogram and is depicted in Figure 3.2. The bandwidth for  $f_1$  and  $f_2$  are assumed to be equal.

The compensating networks used in this study include  $Y_3$  only.  $Y_{3\ hi}$  is furnished by a RL parallel combination and  $Y_{3\ lo}$  is furnished by a single resistance. The arrangement is shown in Figure 3.3.

In each search, the maximum-minimum-reduction criteria is used. The result of this study is summarized in Table 3.1. As seen from this study, there exists definitely a trade-off between the amount of reduction and the bandwidth covered in a particular assumed frequency spread of the interfering signals.

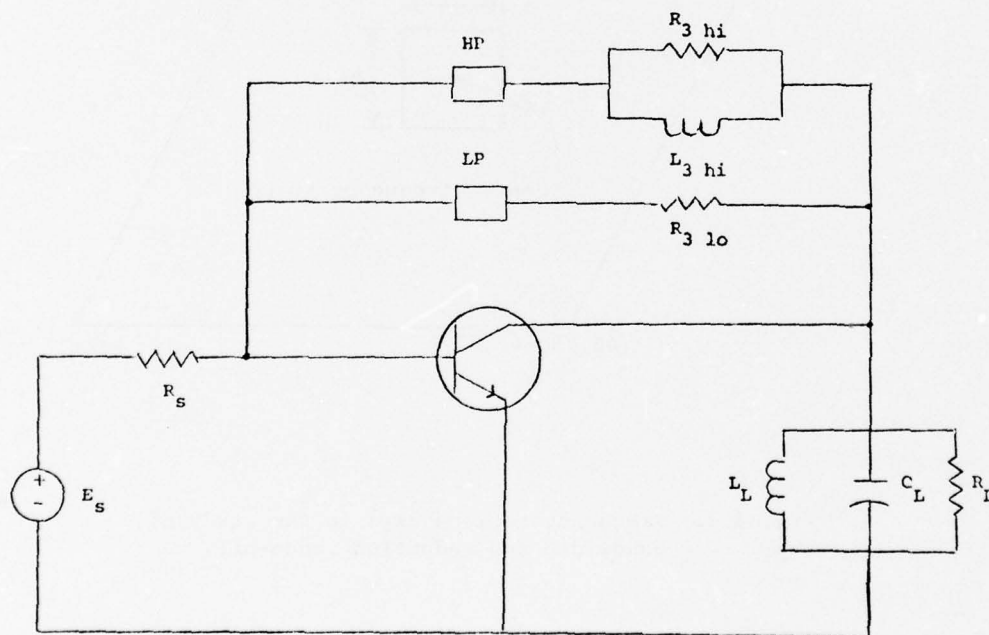


Fig. 3.3. Amplifier with two compensating networks, one of each frequency range.

Table 3.1. Calculated Bandwidth and Reduction Trade-Off

Bandwidth for $f_1$ and $f_2$	Compensating Network Parameters			Minimum Reduction in dB
	$R_{3 \text{ hi}} (\Omega)$	$L_{3 \text{ hi}} (\text{nH})$	$R_{3 \text{ lo}} (\Omega)$	
0.001	17.25	6.039	2.952	75.34
0.01	17.85	6.002	3.651	55.78
0.05	17.71	5.773	1.653	45.43
0.10	18.06	5.883	3.015	39.28
0.15	17.23	5.676	3.317	34.11
0.20	17.35	5.778	2.963	33.76
0.25	17.81	5.992	2.150	33.15
Entire Parallelo- gram of Figure 3.2	17.70	5.756	1.875	32.10

### 3.4. Third-Order Intermodulation Reduction Achievable Using Two Compensating Networks

The frequency region of interest in this chapter is redrawn in Figure 3.4. Numeral designations of key points are used here.

In this study, we shall assume a fixed bandwidth of 0.5 MHz for  $f_2$ . The range of this bandwidth is then varied from one end of the parallelogram to the other. The corresponding range of  $f_1$  is taken to be all the frequencies that will combine with  $f_2$  to give a third-order intermodulation that falls within the pass band of the IF stages. For example, in the first step of this study, we assume

$$47.5 < |f_2| < 47.75 \quad (3.3)$$

and

$$49.75 < |2f_1 + f_2| < 50.25 \quad (3.4)$$

Inequalities (3.3) and (3.4) include the region of the  $f_1$  and  $f_2$  combination bound by the parallelogram 1-2-3-4 of Figure 3.4

In Figure 3.4, the parallelogram bound by 16-19-27-24 can be excluded from the study since the signals themselves will fall within the IF band and, their first-order effects will be much more problematic than their higher-order effects. For this reason, this region is largely by-passed in this study.

The compensating network used is the same as that shown in Figure 3.3.

The result of this study is summarized in Table 3.2.

It is seen from this study that on one side of the center of the parallelogram, approximately the same degree of reduction is achievable

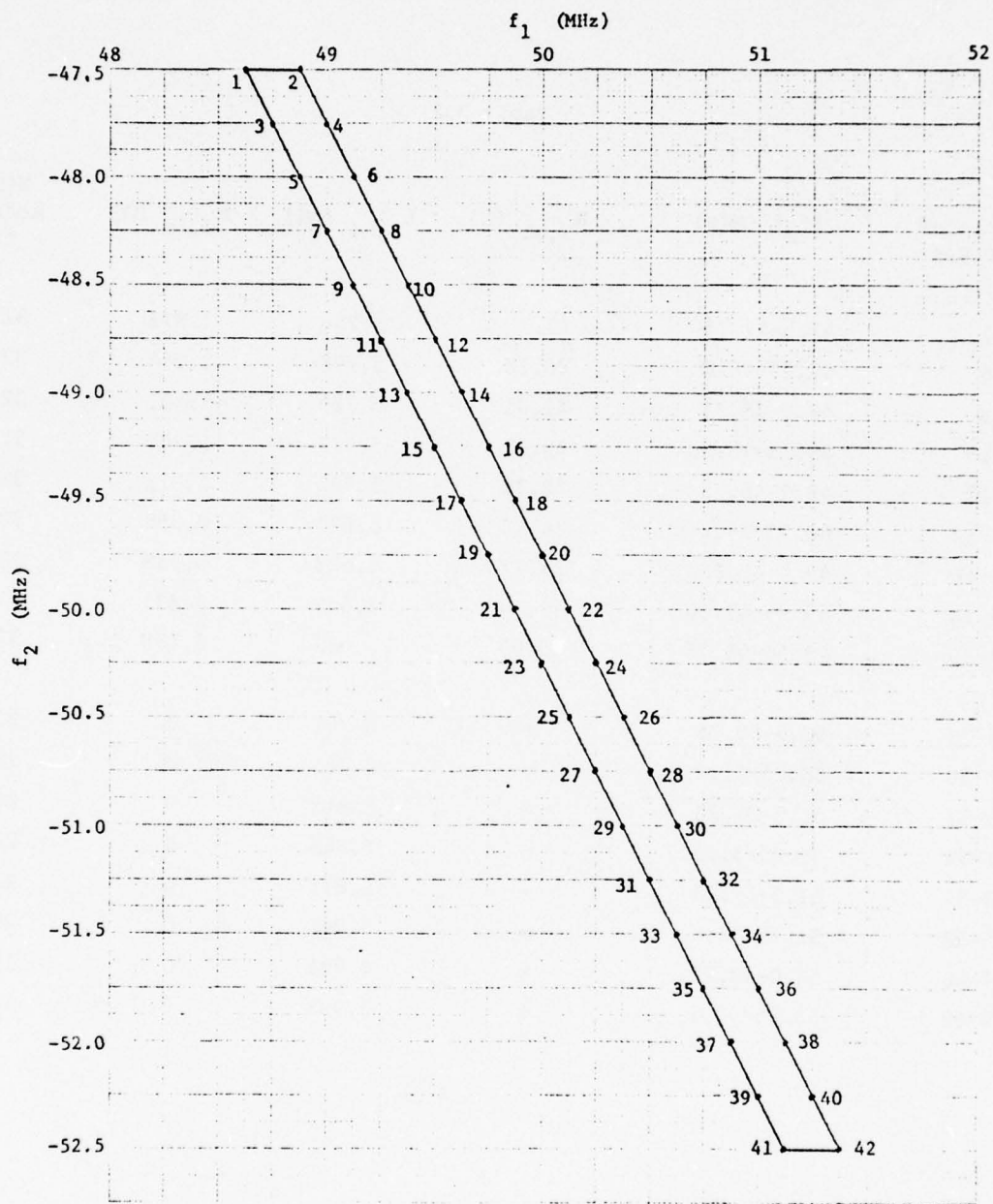


Fig. 3.4. Frequency combinations of point designations.



Table 3.2

Points of Vertexes	$ f_2 $ (MHz)	$R_{3,hi}$ ( $\Omega$ )	$L_{3,hi}$ (nH)	$R_{3,lo}$ ( $\Omega$ )	Minimum Reduction in dB
1-4	47.5-47.75	17.7	5.756	1.875	32.1
3-6	47.75-48.0	20.12	5.798	1.544	32.0
5-8	48.0-48.25	21.01	5.717	1.401	32.5
7-10	48.25-48.5	20.65	5.577	1.307	31.0
9-12	48.5-48.75	23.32	5.598	1.011	31.89
11-14	48.75-49.0	26.18	5.676	0.358	32.97
13-16	49.0-49.25	28.77	5.622	0.338	32.67
15-18	49.25-49.50	40.04	5.644	0.833	33.01
17-20	49.50-49.75	45.05	5.687	0.198	33.44
25-28	50.5-50.75	$\infty$	5.761	0	32.64
27-30	50.75-51.0	$\infty$	5.785	0	28.74
29-32	51.0-51.25	$\infty$	5.818	0	26.00
31-34	51.25-51.5	$\infty$	5.846	0	23.87
33-36	51.5-51.75	$\infty$	5.871	0	22.14
35-38	51.75-52.0	$\infty$	5.890	0	20.67
37-40	52.0-52.25	$\infty$	5.904	0	19.39
39-42	52.25-52.5	$\infty$	5.903	0	18.26

throughout the region for the same frequency spread. As the frequency of  $|f_2|$  is moved to below the center region, the two resistance values approach their limiting values of zero. The reduction begins to diminish. Hence, a slightly more complicated network will have to be used to achieve a comparable reduction for the rest of the parallelogram.

### 3.5. Third-Order Intermodulation Reduction Achievable Using Four Compensating Networks

The same study carried out in Section 3.3 is repeated here except that  $Y_1$  is added to the compensating networks as shown in Figure 3.5.

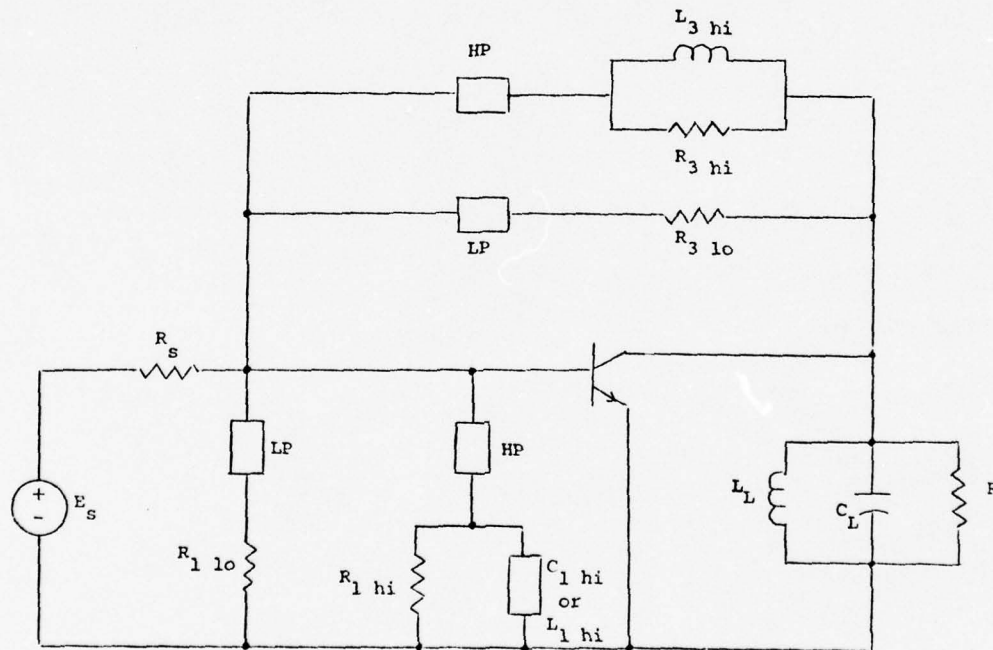


Fig. 3.5. Amplifier with four compensating networks.

The result of this study is summarized in Table 3.3.

It is seen from this result that throughout the top half of the parallelogram, the amount of reduction increased only slightly when  $y_1$  is added to the network. However, throughout the bottom half, the reduction is greatly increased by its addition--to about the same level as the top half.

Table 3.3

Points of Vertexes	$ f_2 $ (MHz)	$R_{3,hi}$ ( $\Omega$ )	$L_{3,hi}$ (nH)	$R_{3,lo}$ ( $\Omega$ )	$R_{1,hi}$ (k $\Omega$ )	$L_{1,hi}$ ( $\mu$ H)	$R_{1,lo}$ ( $\Omega$ )	Minimum Reduction in dB
1-4	47.50-47.75	18.08	5.781	1.487	1.111	11.307	33.35	32.29
3-6	47.75-48.00	18.11	5.684	0.9523	1.047	13.940	38.23	32.28
5-8	48.00-48.25	18.24	5.586	0.6726	0.9425	14.457	42.48	32.50
7-10	48.25-48.50	20.37	5.598	0.5615	1.1561	13.408	26.75	32.02
9-12	48.50-48.75	22.22	5.592	0.5435	1.1710	11.956	25.90	32.23
11-14	48.75-49.00	26.02	5.631	0.4713	1.5576	14.757	17.414	33.92
13-16	49.00-49.25	30.12	5.620	0.4690	1.5649	14.307	17.369	32.84
15-18	49.25-49.50	34.00	5.582	0.4275	1.5949	16.265	32.58	33.04
17-20	49.50-49.75	42.44	5.5998	0.4018	2.0619	17.396	88.87	34.02
$C_{1,hi}$ (pF)								
25-28	50.50-50.75	72.14	5.721	0.1717	1.6207	17.35	32.37	34.23
27-30	50.75-51.00	66.19	5.721	0.1598	1.9084	25.62	35.50	34.69
29-32	51.00-51.25	75.06	5.644	0.1608	1.1013	28.97	30.34	33.69
31-34	51.25-51.50	83.74	5.624	0.8091	1.1834	36.13	30.34	32.77
33-36	51.50-51.75	103.09	5.709	0.4193	1.8018	41.06	27.23	34.92
35-38	51.75-52.00	93.63	5.687	0.4459	1.6447	49.34	23.68	35.37
37-40	52.00-52.25	59.95	5.603	0.5579	1.3369	63.82	2551.0	35.41
39-42	52.25-52.50	69.34	5.523	0.5570	1.0893	67.16	31.88	32.03



## CHAPTER IV

### OTHER TRANSISTOR NONLINEARITIES

#### 4.1. Introduction

So far, we have examined the reduction of third-order intermodulation in a transistor due to its nonlinearity in the emitter resistance only. This was done primarily for two reasons. First, in most transistors, the nonlinear effects due to this resistance are the dominant ones. The other reason is to simplify the computation effort so that the effectiveness of the compensation networks can be more easily assessed.

In a practical situation, nonlinearities other than that in the emitter resistance, cannot be totally ignored. We shall presently discuss the inclusion of other nonlinearities.

#### 4.2 Transistor Nonlinearities

The modelling of transistor nonlinearities suitable for interference study has been well explored [7,8,9]. The general incremental model of a transistor is shown in the dashed box of Figure 4.1. In this circuit the following nonlinearities are included:

- (1) Nonlinear emitter resistance effect is represented by  $k(v_2)$ . This is the only nonlinear effect that was included in the study of Chapters II and III.
- (2) Nonlinear emitter capacitance effect is represented by  $\gamma_e(v_2)$ .
- (3) Nonlinear collector capacitance effect is represented by  $\gamma_c(v_3 - v_2)$ .

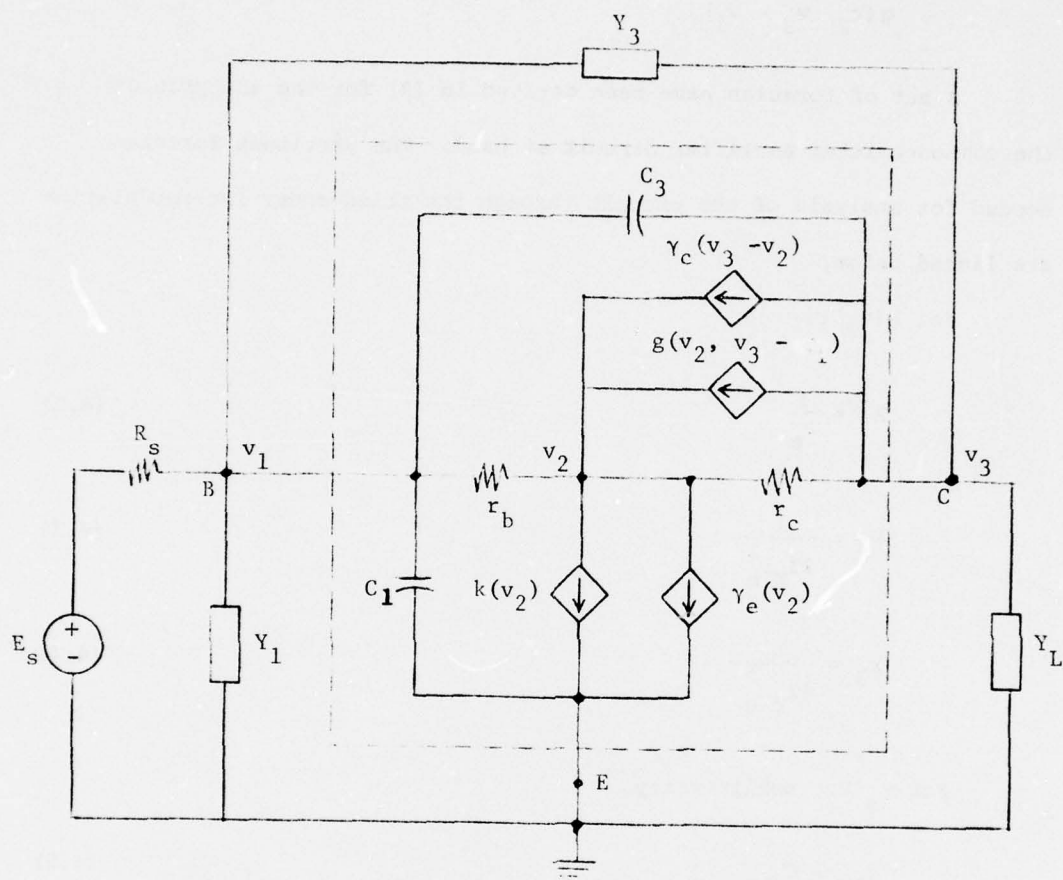


Fig. 4.1. Amplifier circuit with transistor equivalent circuit including all known nonlinearities.

- (4) The nonlinearity associated with  $h_{FE}$  and the avalanche nonlinearity are represented by

$$g(v_2, v_3 - v_1).$$

A set of formulas have been derived in [9] for the analysis of the common-emitter amplifier circuit at hand. The pertinent formulas needed for analysis of the circuit through the third-order intermodulation are listed below.

For  $k(v_2)$ :

$$k_1 = \frac{1}{r_e} \quad (4.2)$$

$$k_2 = \frac{1}{2I_E r_e^2} \quad (4.3)$$

$$k_3 = \frac{1}{6I_E^2 r_e^3} \quad (4.4)$$

For  $\gamma_e(v_2)$  nonlinearity,

$$\gamma_{1e} = C_2 \quad (4.5)$$

$$\gamma_{2e} = \frac{1}{2} C_d' k_1 \quad (4.6)$$

$$\gamma_{3e} = \frac{1}{3} C_d' k_2 \quad (4.7)$$

where  $C_d'$  is that component of  $C_2$  that relates the diffusion capacitance to emitter current.

For  $\gamma_c(v_3 - v_2)$  nonlinearity

$$\gamma_{1c} = C_{1c} \quad (4.8)$$

$$\gamma_{2c} = \frac{\mu}{2! (\phi - V_{CB})} C_c \approx - \frac{\mu}{-2V_{CB}} C_c \quad (4.9)$$

$$\gamma_{3c} = \frac{\mu(\mu+1)}{3! (\phi - V_{CB})^2} C_c \approx \frac{\mu(\mu+1)}{6V_{CB}^2} C_c \quad (4.10)$$

where  $\mu = \frac{1}{3}$  and  $\phi$  is the barrier voltage.

For the  $g(v_2, v_3 - v_1)$ , we have the following series of formulas:

$$h_{FE} = \frac{h_{FE\max}}{1 + a \log^2 \left( \frac{I_C}{I_{C\max}} \right)} \quad (4.11)$$

$$I_{GC} = + m \frac{h_{FE}}{1 + h_{FE}} I_E \quad (4.12)$$

$$b_1 = 1 + h_{FE\max} + a \log^2 \left( \frac{I_{GC}}{I_{C\max}} \right) + 2a \log \left( \frac{I_{GC}}{I_{C\max}} \right) \log \epsilon \quad (4.13)$$

$$b_2 = \frac{a \log \epsilon}{I_{GC}} \left[ \log \left( \frac{I_{GC}}{I_{C\max}} \right) + \log \epsilon \right] \quad (4.14)$$

$$b_3 = - \frac{a \log \epsilon}{3I_{GC}} \log \left( \frac{I_{GC}}{I_{C\max}} \right) \quad (4.15)$$

$$m_0 = \left[ 1 - \left( \frac{V_{CB}}{V_{CBO}} \right)^\eta \right]^{-1} \quad (4.16)$$

$$m_1 = \frac{\eta V_{CB}^{\eta-1}}{V_{CBO}^\eta} - m_0^2 \quad (4.17)$$



$$m_2 = \frac{m_1^2}{m_o} + \frac{1}{2} \frac{(\eta-1)}{V_{CB}} m_1 \quad (4.18)$$

$$m_3 = \frac{2}{3} m_2 \left[ \frac{2m_1}{m_o} + \frac{\eta-1}{2V_{CB}} \right] - \frac{m_1}{3} \left[ \frac{m_1^2}{m_o^2} + \frac{\eta-1}{2V_{CB}} \right] \quad (4.19)$$

$$d_1 = + \frac{h_{FEmax}}{b_1} \quad (4.20)$$

$$d_2 = - \frac{b_2 h_{FEmax}^2}{b_1^3} \quad (4.21)$$

$$d_3 = h_{FEmax}^3 \left[ \frac{2b_2^2 - b_1 b_3}{b_1^5} \right] \quad (4.22)$$

The node equations that govern the relationship of this amplifier is Equation (4.23) which is given on the following page, where  $Y_L$  is the combined admittance of  $K_L$ ,  $C_L$ , and  $L_L$  in parallel.

Denoting the first three orders of nonlinear transfer functions at node 1 to be

$$A_1(f_1), A_2(f_1, f_2), A_3(f_1, f_2, f_3) .$$

those at node 2 to be

$$B_1(f_1), B_2(f_1, f_2), B_3(f_1, f_2, f_3)$$

and those at node 3 to be

$$C_1(f_1), C_2(f_1, f_2), C_3(f_1, f_2, f_3)$$

We have for the first order

$$\begin{aligned}
 [Y(s)] = & \begin{bmatrix} g_s + s(c_1 + c_3) + g_b + y_1 + y_3 & -g_b & -s c_3 - y_3 \\ -g_b + d_1 I_{E1}^m & g_b + g_c + k_1 - d_1 m k + s(\gamma_{1e} + \gamma_{1c}) & -g_c - s \gamma_{1c} - d_1 I_{E1}^m \\ -s c_3 - d_1 I_{E1}^m - y_3 & -g_c - s \gamma_{1c} + d_1 m k & g_c + s c_3 + y_1 + s \gamma_{1c} - d_1 I_{E1}^m + y_3 \end{bmatrix} \\
 & (4.23)
 \end{aligned}$$

$$\begin{bmatrix} A_1(f_1) \\ B_1(f_1) \\ C_1(f_1) \end{bmatrix} = [Y(j2\pi f_1)]^{-1} \begin{bmatrix} g_s \\ 0 \\ 0 \end{bmatrix} \quad (4.24)$$

For higher order analysis, it is expedient to use the following intermediate variables

$$L_{12} = -k_2 - s\gamma_{2e} + d_{1o} m k_2 + d_{2o} m^2 k_1^2$$

$$L_{22} = -k_3 - s\gamma_{3e} + d_{1o} m k_3 + 2d_{2o} m^2 k_1 k_2 + d_{3o} m^3 k_1^3$$

$$L_{32} = s\gamma_{2c}$$

$$L_{42} = s\gamma_{3c}$$

$$L_{52} = d_{1E} I_{m2} + d_{2E} I_{m1}^2$$

$$L_{62} = d_{1o} m k_1 + 2d_{2o} I_{Eo} m m k_1$$

$$L_{72} = d_{1E} I_{m3} + 2d_{2E} I_{m1}^2 m_2 + d_{3E} I_{m1}^3$$

$$L_{82} = d_{12} m k_1 + 2d_{2Eo} I_{Eo} m k_1 m_2 + 2d_{2E} I_{m1}^2 k_1$$

$$L_{92} = d_{1o} m k_2 + 2d_{2Eo} I_{Eo} m m k_2 + 2d_{2o} m k_1^2 m_1$$

$$L_{13} = -L_{12} - k_2 - s\gamma_{2e}$$

$$L_{23} = -L_{22} - k_3 - s\gamma_{3e}'$$

$$L_{33} = -L_{32}$$

$$L_{43} = -L_{42}$$

$$L_{53} = -L_{52}$$

$$L_{63} = -L_{62}$$

$$L_{73} = -L_{72}$$

$$L_{83} = -L_{82}$$

$$L_{93} = -L_{92} \quad (4.25)$$

The second-order transfer functions are given by

$$\begin{bmatrix} A_2(f_1, f_2) \\ B_2(f_1, f_2) \\ C_2(f_1, f_2) \end{bmatrix} = [Y(j2\pi(f_1 + f_2))]^{-1} \begin{bmatrix} 0 \\ \hat{I}_{22}(f_1, f_2) \\ \hat{I}_{32}(f_1, f_2) \end{bmatrix} \quad (4.26)$$

where:

$$\begin{aligned} \hat{I}_{22}(f_1, f_2) = & L_{12}B_1(f_1)B_2(f_2) + L_{32}[C_1(f_1) - B_1(f_1)][C_1(f_2) - B_1(f_2)] \\ & + L_{52}[C_1(f_1) - A_1(f_1)][C_1(f_2) - A_1(f_2)] + L_{62}\{[C_1(f_1) - A_1(f_1)]B_1(f_2)\}_P \end{aligned} \quad (4.27)$$



where the subscript p denotes the average of all possible permutations of the arguments  $f_1$ ,  $f_2$ , and  $f_3$ .  $\hat{I}_{32}(f_1, f_2)$  is identical to  $\hat{I}_{22}$  except  $L_{k2}$  is replaced by  $L_{k3}$ ,  $k = 1, 3, 5, 6$ .

The third-order transfer functions are given by

$$\begin{bmatrix} A_3(f_1, f_2, f_3) \\ B_3(f_1, f_2, f_3) \\ C_3(f_1, f_2, f_3) \end{bmatrix} = [Y(j2\pi(f_1 + f_2 + f_3))]^{-1} \begin{bmatrix} 0 \\ \hat{I}_{23}(f_1, f_2, f_3) \\ \hat{I}_{33}(f_1, f_2, f_3) \end{bmatrix} \quad (4.28)$$

where:

$$\begin{aligned} I_{23}(f_1, f_2, f_3) = & 2L_{12}[B_1(f_1)B_2(f_2, f_3)]_p + L_{22}B_1(f_1)B_1(f_2)B_1(f_3) \\ & + 2L_{32}\{[C_1(f_1) - B_1(f_1)][C_2(f_2, f_3) - B_2(f_2, f_3)]\}_p \\ & + L_{42}[C_1(f_1) - B_1(f_1)][C_1(f_2) - B_1(f_2)][C_1(f_3) - B_1(f_3)] \\ & + 2L_{52}\{[C_1(f_1) - A_1(f_1)][C_2(f_2, f_3) - A_2(f_2, f_3)]\}_p \\ & + L_{62}(\{[C_1(f_1) - A_1(f_1)]B_2(f_2, f_3)\}_p + \{[C_2(f_1, f_2) - A_2(f_1, f_2)]B_1(f_3)\}_p) \\ & + L_{72}[C_1(f_1) - A_1(f_1)][C_1(f_2) - A_1(f_2)][C_1(f_3) - A_1(f_3)] \\ & + L_{82}\{[C_1(f_1) - A_1(f_1)][C_1(f_2) - A_1(f_2)]B_1(f_3)\}_p \\ & + L_{92}\{[C_1(f_1) - A_1(f_1)]B_1(f_2)B_1(f_3)\}_p \end{aligned} \quad (4.29)$$

and  $\hat{I}_{33}(f_1, f_2, f_3)$  is identical to  $\hat{I}_{23}(f_1, f_2, f_3)$  except that  $L_{k2}$  is replaced by  $L_{k3}$  for  $k = 1, 2, 3, \dots, 9$ .

#### 4.3 Numerical Experimentation Including Other Nonlinearities

The transistor amplifier used in the experimentation of Chapters

II and III is further studied with other nonlinearities included. In addition to the parameters given in Chapter II, the following parameters have been assumed:

$$\begin{array}{lll}
 V_{CB} = 10 & \eta = 2 & a = 0.38 \\
 V_{CBO} = 350 & h_{FE_{max}} = 122 & I_C = 0.12 \\
 I_{C_{max}} = 0.633 & I_E = 0.12 & C_d' \approx 0 \\
 C_C = 7 \text{ pF} & \mu = + \frac{1}{3} &
 \end{array}$$

The third-order intermodulation of the amplifier with this transistor is then analyzed along the border of the frequency parallelogram of Figure 3.4 for the case in which only  $r_e$  nonlinearity is included and for the case when  $\gamma_c(v_3 - v_2)$  and  $g(v_2, v_3 - v_1)$  are also included. The results are tabulated in Tables 4.1 and 4.2. It is seen that the difference in neglecting both  $\gamma_c(v_3 - v_2)$  and  $g(v_2, v_3 - v_1)$  nonlinearities varies from approximately 5 dB to 17 dB along the border.

When the compensating networks are applied to the amplifier and when other nonlinearities of the transistor are included, it was found that generally a different set of element values are required for the compensating networks to achieve the optimum effect. It is also noted that the amount of reduction achieved by each compensating network is diminished by roughly the same amount as the difference between the uncompensated third-order intermodulations tabulated in Tables 4.1 and 4.2. In other words, with the proposed compensating scheme, the third-order intermodulation can be reduced to approximately the same absolute level whether we consider the transistor to have  $r_e$  nonlinearity only or when we include  $\gamma_c(v_3 - v_2)$  and  $g(v_2, v_3 - v_1)$  nonlinearities as well.

Table 4.1

THIRD-ORDER TRANSFER FUNCTION WITH  $k(v_2)$  NONLINEARITY ONLY

Point	$f_1$	$f_2$	$f_3$	$f_1+f_2+f_3$	$ C_3(f_1, f_2, f_3) $
	(MHz)				
1	48.625	48.625	-47.50	49.75	.0540039
2	48.875	48.875	-47.50	50.25	.0450855
3	48.750	48.750	-47.75	49.75	.0451635
4	49.000	49.000	-47.75	50.25	.0373721
5	48.875	48.875	-48.00	49.75	.0372144
6	49.125	49.125	-48.00	50.25	.0306464
7	49.000	49.000	-48.25	49.75	.0302171
8	49.250	49.250	-48.25	50.25	.0249244
9	49.125	49.125	-48.50	49.75	.0242135
10	49.375	49.375	-48.50	50.25	.0201911
11	49.250	49.250	-48.75	49.75	.0192247
12	49.500	49.500	-48.75	50.25	.0164035
13	49.375	49.375	-49.00	49.75	.0152528
14	49.625	49.625	-49.00	50.25	.0135028
15	49.500	49.500	-49.25	49.75	.0122907
16	49.750	49.750	-49.25	50.25	.0114398
17	49.625	49.625	-49.50	49.75	.0103343
18	49.875	49.875	-49.50	50.25	.0102091
19	49.750	49.750	-49.75	49.75	.0093823
20	50.000	50.000	-49.75	50.25	.0098627
21	49.875	49.875	-50.00	49.75	.0094042
22	50.125	50.125	-50.00	50.25	.0104638
23	50.000	50.000	-50.25	49.75	.0103129
24	50.250	50.250	-50.25	50.25	.0120072
25	50.125	50.125	-50.50	49.75	.0119959
26	50.375	50.375	-50.50	50.25	.0144008
27	50.250	50.250	-50.75	49.75	.0143596
28	50.500	50.500	-50.75	50.25	.0175213
29	50.375	50.375	-51.00	49.75	.0173376
30	50.625	50.625	-51.00	50.25	.0212428
31	50.500	50.500	-51.25	49.75	.0208759
32	50.750	50.750	-51.25	50.25	.0254517
33	50.625	50.625	-51.50	49.75	.0249203
34	50.875	50.875	-51.50	50.25	.0300476
35	50.750	50.750	-51.75	49.75	.0294125
36	51.000	51.000	-51.75	50.25	.0349429
37	50.875	50.875	-52.00	49.75	.0342902
38	51.125	51.125	-52.00	50.25	.0400632
39	51.000	51.000	-52.25	49.75	.0394890
40	51.250	51.250	-52.25	50.25	.0453462
41	51.125	51.125	-52.50	49.75	.0449455
42	51.375	51.375	-52.50	50.25	.0507400

Table 4.2

THIRD-ORDER TRANSFER FUNCTION WITH  $k(v_2)$ ,  $\gamma_c(v_3-v_2)$ AND  $g(v_2, v_3-v_1)$  NONLINEARITIES

Point	$f_1$	$f_2$	$f_3$	$f_1+f_2+f_3$	$ C_3(f_1, f_2, f_3) $
	(MHz)				
1	48.625	48.625	-47.50	49.75	.0075294
2	48.875	48.875	-47.50	50.25	.0072248
3	48.750	48.750	-47.75	49.75	.0070008
4	49.000	49.000	-47.75	50.25	.0071659
5	48.875	48.875	-48.00	49.75	.0067372
6	49.125	49.125	-48.00	50.25	.0071531
7	49.000	49.000	-48.25	49.75	.0065613
8	49.250	49.250	-48.25	50.25	.0070711
9	49.125	49.125	-48.50	49.75	.0063676
10	49.375	49.375	-48.50	50.25	.0068776
11	49.250	49.250	-48.75	49.75	.0061216
12	49.500	49.500	-48.75	50.25	.0065823
13	49.375	49.375	-49.00	49.75	.0058433
14	49.625	49.625	-49.00	50.25	.0062308
15	49.500	49.500	-49.25	49.75	.0055873
16	49.750	49.750	-49.25	50.25	.0058919
17	49.625	49.625	-49.50	49.75	.0054225
18	49.875	49.875	-49.50	50.25	.0056435
19	49.750	49.750	-49.75	49.75	.0054045
20	50.000	50.000	-49.75	50.25	.0055507
21	49.875	49.875	-50.00	49.75	.0055503
22	50.125	50.125	-50.00	50.25	.0056412
23	50.000	50.000	-50.25	49.75	.0058313
24	50.250	50.250	-50.25	50.25	.0058953
25	50.125	50.125	-50.50	49.75	.0061893
26	50.375	50.375	-50.50	50.25	.0062590
27	50.250	50.250	-50.75	49.75	.0065609
28	50.500	50.500	-50.75	50.25	.0066698
29	50.375	50.375	-51.00	49.75	.0068937
30	50.625	50.625	-51.00	50.25	.0070752
31	50.500	50.500	-51.25	49.75	.0071539
32	50.750	50.750	-51.25	50.25	.0074411
33	50.625	50.625	-51.50	49.75	.0073285
34	50.875	50.875	-51.50	50.25	.0077544
35	50.750	50.750	-51.75	49.75	.0074264
36	51.000	51.000	-51.75	50.25	.0080222
37	50.875	50.875	-52.00	49.75	.0074795
38	51.125	51.125	-52.00	50.25	.0082715
39	51.000	51.000	-52.25	49.75	.0075435
40	51.250	51.250	-52.25	50.25	.0085468
41	51.125	51.125	-52.50	49.75	.0076953
42	51.375	51.375	-52.50	50.25	.0089056



## CHAPTER V

### COMPUTATION OF COMPENSATING NETWORK PARAMETERS

#### 5.1 Introduction

In the course of this study, several computation techniques have been employed. Initially, we relied heavily on the following strategy:

- (1) Choose a compensation network function a priori.
- (2) Derive the cost function in terms of the amplifier circuit parameters and the compensation network function parameters.
- (3) Establish a criterion by which the cost function is to be minimized.
- (4) Employ the modified Fletcher-Power method to minimize the cost function.
- (5) Synthesize the compensating network.

This strategy turned out to have several drawbacks:

- (a) It is generally difficult to know the proper choice of a starting point which is very vital to the success of the optimization program.
- (b) It is necessary to derive the derivative of the cost function with respect to the compensation network parameter. This step usually requires a great deal of human time and the expressions have to

be completely altered when a network is modified or replaced.

As our numerical experimentation progressed, it became more clear that once we know a good start point the problem is practically solved because the improvement achieved after the proper starting point has been found is usually very minor. Hence, our later strategy really concentrated on the search for a good starting point. The improvement thereafter is achieved mainly by a systematic search routine.

This last strategy is adopted partly because our experience showed that with this particular compensation technique, the complexity of the compensating network buys us very little, if any, improvement in intermodulation reduction. Hence, it is most expedient to use the simplest compensating network possible.

In the context of this background information, the following sections describe the most practical computational strategy for determining the best passive compensating network.

## 5.2 Calculation of Third-Order Intermodulation

The heart of the computational effort is the basic third-order transfer function analysis routine for a given amplifier. The main program is shown below.

```
PROGRAM INTANA(INPUT,OUTPUT,TAPE5=INPUT,TAPE6=OUTPUT)
REAL K1,K2,K3,IC,ICM,IE,IGC
COMPLEX IA1,IB1,IC1,IA2,IB2,IC2,IA3,IB3,IC3
COMPLEX VAF1,VAF2,VAF3,VBF1,VBF2,VBF3,VCF1,VCF2,VCF3
COMPLEX VCAF1,VCAF2,VCAF3,VCBF1,VCBF2,VCBF3
COMPLEX VAF12,VAF13,VAF23,VBF12,VBF13,VBF23,VCF12,VCF13,VCF23
COMPLEX VCAF12,VCAF13,VCAF23,VCBF12,VCBF13,VCBF23
COMPLEX VAF123,VBF123,VCF123
COMMON II1,F1,F2,F3,RE,PG,GX,GY
```

```

C      READ IN ANY NUMBER OF SETS OF FREQUENCY COMBINATIONS

      II1=3
777  READ(5,*) F1,F2,F3
      IF(EOF(5)) 77,20
20   II1=II1+1

C      ASSIGN TRANSISTOR AND CIRCUIT PARAMETERS

      VG=1.0
      RG=75.0
      CLE=0.4342944829032
      VCB=10.0
      N=2
      A=0.38
      VCB0=350.0
      HFEM=122.0
      IC=0.12
      ICM=0.633
      IE=0.12
      RE=0.2165

C      START COMPUTATION OF INTERMEDIATE PARAMETERS

      PAI=3.141592654
      CLE=0.4342944829032
      K1=1./RE
      K2=1./(2.*IE*RE**2)
      K3=1./(6.*IE**2*RE**3)
      GAM2C=-0.14341085E-12
      GAM3C=2.80432E-14
      HFE=HFEM/(1+A*(ALOG10(IC/ICM)**2))
      IGC=CM*HFE*IE/(1+HFE)
      B1=1+HFEM+A*(ALOG10(IGC/ICM)**2)+2*A*CLE*ALOG10(IGC/ICM)
      B2=A*CLE/IGC*(ALOG10(IGC/ICM)+CLE)
      B3=-A*CLE/(3*IGC**2)*ALOG10(IGC/ICM)
      CM0=1/(1-(VCB/VCB0)**N)
      CM1=N*VCB**(N-1)*CM0*CM0/(VCB0**N)
      CM2=CM1*CM1/CM0+0.5*(N-1)*CM1/VCB
      CM3=2*CM2/3*(2*CM1/CM0+(N-1)*0.5/VCB)-CM1/3*((CM1/CM0)**2
1+(N-1)/2/VCB/VCB)
      D1=-HFEM/B1
      D1=-D1
      D2=-B2*HFEM*HFEM/(B1**3)
      D3=HFEM**3*((B1*B3-2*B2*B2)/(B1**5))
      D3=-D3
      GX=D1*CM0*K1
      GY=D1*IE*CM1
      E12=-K2 + D1*CM0*K2 + D2*CM0**2*K1**2
      E22=-K3 +D1*CM0*K3 + 2*D2*CM0**2*K1*K2 +D3*CM0**3*K1**3
      E52= D1*IE*CM2 + D2*IE**2*CM1**2
      E62= D1*CM1*K1 + 2*D2*IE*CM0*CM1*K1
      E72= D1*IE*CM3 +2*D2*IE**2*CM1*CM2 +D3*IE**3*CM1**3
      E82= D1*CM2*K1 +2*D2*IE*CM0*K1*CM2 +2*D2*IE*CM1**2*K1

```

E92= D1\*CM1\*K2 +2\*D2\*IE\*CMJ\*CM2\*K2 +2\*D2\*CMO\*K1\*\*2\*CM1

C ANALYSIS OF FIRST-ORDER CIRCUIT

IA1=CMPLX(VG/RG, 0.0)  
 IB1=CMPLX(0.0, 0.0)  
 IC1=CMPLX(0.0, 0.0)  
 F=F1  
 CALL GFIFVB(F,IA1,IB1,IC1,VAF1,VBF1,VCF1)  
 F=F2  
 CALL GFIFVB(F,IA1,IB1,IC1,VAF2,VBF2,VCF2)  
 F=F3  
 CALL GFIFVB(F,IA1,IB1,IC1,VAF3,VBF3,VCF3)

C ANALYSIS OF SECOND ORDER CIRCUIT

VCBF1=VCF1-VBF1  
 VCBF2=VCF2-VBF2  
 VCBF3=VCF3-VBF3  
 VCAF1=VCF1-VAF1  
 VCAF2=VCF2-VAF2  
 VCAF3=VCF3-VAF3  
 F=F1+F2  
 E32= CMPLX(0.0,2\*PAI\*F)\*GAM2C  
 IA2=CMPLX(0.0, 0.0)  
 IB2=E12\*VBF1\*VBF2 + E32\*VCBF1\*VCBF2 + E52\*VCAF1\*VCAF2  
 1 + E62\*(VCAF1\*VBF2+VCAF2\*VBF1)/2  
 IC2=-IB2 - K2\*VBF1\*VBF2  
 CALL GFIFVB(F,IA2,IB2,IC2,VAF12,VBF12,VCF12)  
 F=F1+F3  
 E32= CMPLX(0.0,2\*PAI\*F)\*GAM2C  
 IB2=E12\*VBF1\*VBF3 + E32\*VCBF1\*VCBF3 + E52\*VCAF1\*VCAF3  
 1 + E62\*(VCAF1\*VBF3+VCAF3\*VBF1)/2  
 IC2=-IB2 - K2\*VBF1\*VBF3  
 CALL GFIFVB(F,IA2,IB2,IC2,VAF13,VBF13,VCF13)  
 F=F2+F3  
 E32= CMPLX(0.0,2\*PAI\*F)\*GAM2C  
 IB2=E12\*VBF2\*VBF3 + E32\*VCBF2\*VCBF3 + E52\*VCAF2\*VCAF3  
 1 + E62\*(VCAF2\*VBF3+VCAF3\*VBF2)/2  
 IC2=-IB2 - K2\*VBF2\*VBF3  
 CALL GFIFVB(F,IA2,IB2,IC2,VAF23,VBF23,VCF23)

C ANALYSIS OF THIRD-ORDER CIRCUIT

F=F1+F2+F3  
 E32= CMPLX(0.0,2\*PAI\*F)\*GAM2C  
 E42= CMPLX(0.0,2\*PAI\*F)\*GAM3C  
 VCBF12=VCF12-VBF12  
 VCBF13=VCF13-VBF13  
 VCBF23=VCF23-VBF23  
 VCAF12=VCF12-VAF12  
 VCAF23=VCF23-VAF23  
 VCAF13=VCF13-VAF13  
 IA3=CMPLX(0.0, 0.0)  
 IB3=2\*E12\*(VBF1\*VBF23+VBF2\*VBF13+VBF3\*VBF12)/3  
 1 +E22\*VBF1\*VBF2\*VBF3  
 1 +2\*E32\*(VCBF1\*VCBF23+VCBF2\*VCBF13+VCBF3\*VCBF12)/3  
 1 +E42\*VCBF1\*VCBF2\*VCBF3





```

1      +2*E52*(VCAF1*VCAF23+VCAF2*VCAF13+VCAF3*VCAF12)/3
1      +262*(VCAF1*VBF23+VCAF2*VBF13+VCAF3*VBF12)/3
1      +262*(VCAF12*VBF3+VCAF13*VBF2+VCAF23*VBF1)/3
1      +E72*VCAF1*VCAF2*VCAF3
1      +E82*(VCAF1*VCAF2*VBF3+VCAF2*VCAF3*VBF1+VCAF1*VCAF3*VBF2)/3
1      +E92*(VCAF1*VBF2*VBF3+VCAF2*VBF1*VBF3+VCAF3*VBF1*VBF2)/3
IC3=-IB3-2.*K2*(VBF1*VBF23+VBF2*VBF13+VBF3*VBF12)/3
1      -K3*VBF1*VBF2*VBF3
CALL GFIFVB(F,IA3,IB3,IC3,VAF123,VBF123,VCF123)

```

C VCF123 IS THE THIRD-ORDER TRANSFER FUNCTION

GO TO 777

77 STOP  
END

C SUBROUTINE GFIFVB(F,IA,IB,IC,VA,VB,VC)  
THIS SUBROUTINE FINDS THE NCCF VOLTAGES AT THE FREQUENCY F  
C WHEN THE SOURCE CURRENTS IA, IB, IC, AND THE Y MATRIX ARE GIVEN  
DIMENSION JC(4)  
REAL LL,L5  
COMPLEX IA,IB,IC,VA,VB,VC  
COMPLEX YGAM1C,YGX,YGY,Y1,Y2,YRB,YRC,YRE,YRL,YC1,YC2,YC3,YCL,YLL,YL  
COMPLEX Y(3,4)  
COMMON I11,F1,F2,F3,RC,RG,GX,GY

C ASSIGN ADDITIONAL TRANSISTOR AND CIRCUIT VALUES

```

C1=6.0E-12
C2=1.5E-9
C3=9.0E-12
RB=13.6
RC=5200.
GAM1C=7.0E-12
CL=1.193757E-9
LL=8.526156E-9
RL=75.0

```

C START CALCULATION OF ADMITTANCES

```

W=2.0*3.141592654*F
YGAM1C=CMPLX(0.,W*GAM1C)
YGX=CMPLX(GX,0.)
YGY=CMPLX(GY,0.)
YRG=CMPLX(1.0/RG, 0.0)
Y1=CMPLX(0.0, 0.0)
Y3=CMPLX(0.0,0.0)
YRB=CMPLX(1.0/RB, 0.0)
YRC=CMPLX(1.0/RC, 0.0)
YRE=CMPLX(1.0/RE, 0.0)
YRL=CMPLX(1.0/RL, 0.0)
YC1=CMPLX(0.0, W*C1)
YC2=CMPLX(0.0, W*C2)
YC3=CMPLX(0.0, W*C3)
YCL=CMPLX(0.0, W*CL)
YLL=CMPLX(0.0, -1.0/(W*LL))
YL=YRL+YCL+YLL

```

C ASSIGN VALUES TO NODAL ADMITTANCE MATRIX

```
Y(1,1)=YRG+YL+YC1+YRB+Y3+YC3
Y(1,2)=-YRB
Y(1,3)=-Y3-YC3
Y(1,4)=IA
Y(2,1)=-YRB+YGY
Y(2,2)=YRB+YRE+YC2+YRC+YGAM1C-YGX
Y(2,3)=-YRC -YGAM1C-YGY
Y(2,4)=IB
Y(3,1)=-Y3-YC3-YGY
Y(3,2)=-YRC-YGAM1C+YGX
Y(3,3)=Y3+YC3+YRC+YRL+YL+YGAM1C+YGY
Y(3,4)=IC
```

C CALL SUBROUTINE TO SOLVE MATRIX EQUATION

```
V=(7.0, 0.0)
CALL CGJR(Y,4,3,3,4,JC,V),RETURNS(44)
```

C THE THREE NODE VOLTAGES ARE

```
VA=Y(1,4)
VB=Y(2,4)
VC=Y(3,4)
```

```
GO TO 77
44 CONTINUE
WRITE(6,15) F ,JC(1)
15 FORMAT(/4X,F10.2,4X,6HJC(1)=,I4,4X,10HBAD MATRIX)
STOP
77 RETURN
END
```

The relationships used in this program are those included in Chapter IV. For the analysis of the transfer functions when  $r_e$  non-linearity only is considered, such as was done in Chapters II and III, we only need to set certain parameters to zero.

Subroutine CGJR is a library program which is used to solve a set of linear simultaneous equations using Gauss-Jordan reduction method. The print-out and a description of this subroutine is included in Appendix A.

Most of the variables used in the Fortran program use the same combination of alphanumeric characters used in Chapter IV. Those that are different are listed below:

$CLF = \log \epsilon$   
 $GAM1C = \gamma_{1c}$   
 $GAM2C = \gamma_{2c}$   
 $GAM3C = \gamma_{3c}$   
 $CM0 = m_0$   
 $CM1 = m_1$   
 $CM2 = m_2$   
 $CM3 = m_3$   
 $F12 = L_{12}$   
 $F22 = L_{22}$   
 $F32 = L_{32}$   
 $F42 = L_{42}$   
 $F52 = L_{52}$   
 $F62 = L_{62}$   
 $F72 = L_{72}$   
 $F82 = L_{82}$   
 $F92 = L_{92}$   
 $VAF1 = A_1(f_1)$   
 $VBF1 = B_1(f_1)$   
 $VAF12 = A_2(f_1, f_2)$   
 $VBF23 = B_2(f_2, f_3)$   
 $VCF123 = C_3(f_1, f_2, f_3)$

### 5.3 Interactive Mode Search for Values of $Y_1$ and $Y_3$ at One Frequency Combination

To search for the appropriate compensating networks, it is found most efficient to first find the best values for  $Y_{1 \text{ hi}}$ ,  $Y_{1 \text{ lo}}$ ,  $Y_{3 \text{ hi}}$ , and  $Y_{3 \text{ lo}}$  for the frequency combination corresponding to the center of the

region occupied by the bandwidths of the two interfering signals. The third-order transfer function is first calculated using the program listed in Section 5.2 at this center frequency. The magnitude of this transfer function is entered as H30 in this new program. The variables Q(1),Q(2), . . . ,Q(8) are the real and imaginary parts of the four admittances mentioned above. The program is a modification of the Analysis Program listed on page 65 and only new key statements are listed below.

```

      .
      .
      .
      DIMENSION Q(8)
      .
      .
      .
C     ASSIGN SIGNAL FREQUENCIES
      F1=
      F2=F1
      F3=

C     GIVE VALUE OF THIRD-ORDER TRANSFER FUNCTION WITHOUT Y1 AND Y3
      H30=

C     ASSIGN INITIAL VALUES FOR THE VARIABLES
      Q(1)=
      Q(2)=
      Q(3)=
      Q(4)=
      Q(5)=
      Q(6)=
      Q(7)=
      Q(8)=

8877  CONTINUE

      VG=1.0
      .
      .
      .

```



```

CALL GFIFV3(F,IA3,IB3,IC3,VAF123,VBF123,VCF123)

C   COMPUTE AND PRINT REDUCTION IN THIRD-ORDER TRANSFER FUNCTION

H3=SQRT(REAL(VCF123)**2+AIMAG(VCF123)**2)
D3=20.3*ALOG10(H3/H2)
WRITE(6,*) (Q(JJ),JJ=1,8),D3

C   ENTER NEW VALUE OF Q(JJ)
READ(5,*) NJ,QV
Q(NJ)=QV
GO TO 8877
STOP
END

SUBROUTINE GFIFV3(F,IA,IB,IC,VA,VB,BC)
.
.
.

YRG=CMPLX(1.0/P3,0.0)

C   ASSIGN VARIABLE VALUES TO Y1 AND Y3

IF(ABS(W).GT.0.328.AND.ABS(W).LT.1.E8) GO TO 119
IF(ABS(W).LT.0.328) GO TO 117
C   REAL AND IMAGINARY PARTS OF Y1 AND Y3 AT HIGH FREQUENCY
Y1R=Q(1)

Y1I=Q(2)
Y3R=Q(3)
Y3I=Q(4)
GO TO 118
C   REAL AND IMAGINARY PARTS OF Y1 AND Y3 AT LOW FREQUENCY
117 Y1R=Q(5)
Y1I=Q(6)
Y3R=Q(7)
Y3I=Q(8)
118 CONTINUE
Y1=CMPLX(Y1R,Y1I)
Y3=CMPLX(Y3R,Y3I)
GO TO 120
119 Y1=CMPLX(1.0,0.0)
Y3=CMPLX(0.0,0.0)
120 CONTINUE

YRB=CMPLX(1.0/P3,0.0)
.
.
.
.

```

A set of initial values are assigned in the main program. Then these values can be changed one at a time. After each change, the reduction (in dB) and the values of all eight variables are printed out. The variation of this reduction is observed as the Q's are being varied. By judiciously adjusting the values of Q's, the reduction is gradually increased. A section of the print-out of a sequence of such interactive steps is shown below.

NEW Q(1)= 0.053

Q'S: .0530 7.7770 .0000 .6800 .1735 .0054 .0892 .0000  
REDUCTION IS 25.33 DB

NEW Q(3)= 0.0011

Q'S: .0530 7.7770 .0011 .6800 .1735 .0054 .0892 .0000  
REDUCTION IS 25.78 DB

#### 5.4 Automatic Research for Values of $Y_1$ and $Y_3$ At One Frequency Combination

Once the interactive mode of search has rendered a set of values of  $Y_1$  and  $Y_3$ , that gives a reasonably good reduction in third-order transfer function, these values are best readjusted by an automatic search scheme to further increase the reduction. Although several automatic search schemes, such as the Rosenbruck's technique, have been tried, it was finally decided to simply perturb the variables by certain amounts and the reduction computed for each combination of the perturbed variables values. As each reduction is computed, the new set of variable values and reduction is printed out only if the reduction is higher than the highest reduction obtained previously. Thus, after each

perturbation, only the best result is kept. The process is then repeated using the best result as the new starting point. The process is considered complete either when the reduction is extremely high or when the smallest perturbation does not alter the reduction.

The algorithm used is shown below. It is again the same program listed on page 65 with some modifications. Again, only key statements are listed here.

```

      .
      .
      .
      .
      .
C     ASSIGN SIGNAL FREQUENCIES

      F1=
      F2=F1
      F3=

C     ASSIGN TRANSISTOR AND CIRCUIT PARAMETERS

      VG=1.0
      .
      .
      .
      .
      E92=D1*CM1*K2 +2*D2*IE*CM0*CM2*K2 +2*D2*CM3*K2**2*CM1

C     GIVE VALUE OF THIRD-ORDER TRANSFER FUNCTION WITHOUT Y1 AND Y3

      H3Q=

C     READ INITIAL VARIABLE VALUES

      READ(5,*) Q1,Q2,Q3,Q4,Q5,Q6,Q7,Q8

C     SET INITIAL REDUCTION REFERENCE IN DB

      EPSI=-10.0

C     READ IN THE NUMBER OF PERTURBATIONS OF EACH VARIABLE

88    READ(5,*) NM

C     READ IN THE INCREMENT OF PERTURBATION IN PERCENT

      READ(5,*) PQ

```

C COMPUTE AND SET LCOPS FOR VARIABLE VALUE CHANGES

KK=(NM+1)/2  
PGJ =1.0+PQ/100.0

DO 7001 J1=1,NM  
Q(1)=(Q1/(PGJ\*\*KK))\*(PGJ\*\*J1)  
DO 7001 J2=1,NM  
Q(2)=(Q2/(PGJ\*\*KK))\*(PGJ\*\*J2)  
DO 7001 J3=1,NM  
Q(3)=(Q3/(PGJ\*\*KK))\*(PGJ\*\*J3)  
DO 7001 J4=1,NM  
Q(4)=(Q4/(PGJ\*\*KK))\*(PGJ\*\*J4)  
DO 7001 J5=1,NM  
Q(5)=(Q5/(PGJ\*\*KK))\*(PGJ\*\*J5)  
DO 7001 J6=1,NM  
Q(6)=(Q6/(PGJ\*\*KK))\*(PGJ\*\*J6)  
DO 7001 J7=1,NM  
Q(7)=(Q7/(PGJ\*\*KK))\*(PGJ\*\*J7)  
DO 7001 J8=1,NM  
Q(8)=(Q8/(PGJ\*\*KK))\*(PGJ\*\*J8)

C FIRST-ORDER CIRCUIT

.  
.  
.

C SECOND ORDER CIRCUIT

.  
.  
.

C THIRD-ORDER CIRCUIT

.  
.  
.

CALL GFIFVB(F,IA3,IB3,IC3,VAF123,V9F123,VCF123)

C COMPUTE REDUCTION IN THIRD-ORDER TRANSFER FUNCTION

H3=SQRT(REAL(VCF123)\*\*2+AIMAG(VCF123)\*\*2)  
DB=20.0\*ALOG10(H3/H30)

C IF DB INCREASES, PRINT NEW Q'S AND NEW DB

IF(DB.LT.EPSI) GO TO 7001  
EPSI=SAML  
WRITE(6,\*) (Q(JJ),JJ=1,8),DB

C STORE NEW Q'S TEMPORARILY

Q11=Q(1)  
Q22=Q(2)  
Q33=Q(3)  
Q44=Q(4)  
Q55=Q(5)  
Q66=Q(6)  
Q77=Q(7)  
Q88=Q(8)



7001 CONTINUE

C TO TERMINATE PROGRAM, KEY IN 1; OTHERWISE ANY OTHER INTEGER

READ(5,\*) KEN  
IF(KEN.EQ.1) GO TO 98

C USE NEW Q'S TO REPEAT THE PERTURBATION

Q1=Q11  
Q2=Q22  
Q3=Q33  
Q4=Q44  
Q5=Q55  
Q6=Q66  
Q7=Q77  
Q8=Q88  
GO TO 83

98 CONTINUE

STOP  
END

SUBROUTINE GFIFVB(F,IA,IB,IC,VA,VB,VC)

.  
.  
.  
.  
.  
.

#### 5.5 Automatic Search for Maximum Reduction Over a Region of Frequency Combinations

Once the best values for  $Y_{1\text{ lo}}$ ,  $Y_{1\text{ hi}}$ ,  $Y_{3\text{ lo}}$ , and  $Y_{3\text{ hi}}$ , for the center of a region has been obtained, a search for network parameters to maximize the reduction of third-order intermodulation over a region of combinations of frequencies can be made. Based on the findings of Chapters III and IV, it is best to assume as simple a passive network as possible. The simplest network is obviously either an RC or an RL parallel combination depending on whether the imaginary of the admittance is negative or positive. The admittances of these assumed circuits are then inserted into the search program.

In addition to replacing the fixed admittance values by those of simple circuits, the search must be carried out over the entire region. Again, based on the findings of previous chapters, as long as the frequency region is a polygon (typically, a rectangle or a parallelogram), only points at the vertexes need be included in the search. Hence, the only other modification required is to include another loop so that a number of frequency points is included in the search instead of a single point.

Although the search can be done in either the interactive mode or the perturbation mode, in most cases, the former is not necessary if a search for the center point has already been conducted. A print-out of key steps of this program is listed below.

```

      .
      .
      .
      DIMENSION F1(4), F3(4), H30(4), OS(4)
      .
      .
      .
C     GIVE VALUES OF 3RD-ORDER TRANSFER FUNCTION WITHOUT Y1 AND Y2
C     AT THE VERTEXES

      DATA H30/625.0, 624.3, 673.4, 655.9/

C     ASSIGN SIGNAL FREQUENCIES AT THE VERTEXES

      F1(1)=3.4999
      F1(2)=9.5001
      F3(1)=-8.9999
      F3(3)=-3.0001
      F1(3)=F1(1)
      F1(4)=F1(2)
      F3(2)=F3(1)
      F3(4)=F3(3)

```

```

C    ASSIGN TRANSISTOR AND CIRCUIT PARAMETERS
VG=1.0
.
.
.
.
EQ2=C1*CM1*K2 +2*D2*IE*CM0*CM2*K2 +2*D2*CMJ*K2**2*CM1
C    READ INITIAL VARIABLE VALUES
READ(5,*) Q1,Q2,Q3,Q4,Q5,Q6,Q7,Q8
C    SET INITIAL REDUCTION REFERENCE IN DB
EPSI=-10.0
C    READ IN THE NUMBER OF PERTURBATIONS OF EACH VARIABLE
83  READ(5,*) NM
C    READ IN THE INCREMENT OF PERTURBATION IN PERCENT
READ(5,*) PQ
C    COMPUTE AND SET LOOPS FOR VARIABLE VALUE CHANGES
KK=(NM+1)/2
PQJ =1.0+PQ/100.0
DO 7001 J1=1,NM
Q(1)=(Q1/(PQJ**KK))*(PQJ**J1)
DO 7001 J2=1,NM
Q(2)=(Q2/(PQJ**KK))*(PQJ**J2)
DO 7001 J3=1,NM
Q(3)=(Q3/(PQJ**KK))*(PQJ**J3)
DO 7001 J4=1,NM
Q(4)=(Q4/(PQJ**KK))*(PQJ**J4)
DO 7001 J5=1,NM
Q(5)=(Q5/(PQJ**KK))*(PQJ**J5)
DO 7001 J6=1,NM
Q(6)=(Q6/(PQJ**KK))*(PQJ**J6)
DO 7001 J7=1,NM
Q(7)=(Q7/(PQJ**KK))*(PQJ**J7)
DO 7001 J8=1,NM
Q(8)=(Q8/(PQJ**KK))*(PQJ**J8)
C    SET LOOP FOR COMPUTING REDUCTION AT FOUR VERTEXES
DO 7002 NM=1,4

```

```

C      FIRST-ORDER CIRCUIT
      .
      .
C      SECOND ORDER CIRCUIT
      .
      .
C      THIRD-ORDER CIRCUIT
      .
      .
      CALL GFIFVB(F, IAS, IRS, IOS, VAF123, VBF123, VCF123)
C      COMPUTE REDUCTION IN THIRD-ORDER TRANSFER FUNCTION
      H3=SQRT(REAL(VCF123)**2+AIMAG(VCF123)**2)
      DB(NN)=20.0*ALOG10(H3/H30(NN))
7002  CONTINUE
C      IF MINIMUM DB INCREASES, PRINT NEW Q'S AND NEW DB
      DBMIN=AMIN1(DB(1),DB(2),DB(3),DB(4))
      IF(DBMIN.LT.EPSI) GO TO 7001
      EPSI=DBMIN
      WRITE(6,*) (Q(JJ),JJ=1,8),DB
C      STORE NEW Q'S TEMPORARILY
      Q11=Q(1)
      Q22=Q(2)
      Q33=Q(3)
      Q44=Q(4)
      Q55=Q(5)
      Q66=Q(6)
      Q77=Q(7)
      Q88=Q(8)
7001  CONTINUE
C      TO TERMINATE PROGRAM, KEY IN 1; OTHERWISE ANY OTHER INTEGER
      READ(5,*) KEN
      IF(KEN.EQ.1) GO TO 98
C      USE NEW Q'S TO REPEAT THE PERTURBATION
      Q1=Q11
      Q2=Q22
      Q3=Q33
      Q4=Q44

```



Reproduced from  
best available copy.

Q5=Q55  
Q6=Q66  
Q7=Q77  
Q8=Q88  
GO TO 98

98 CONTINUE

STOP  
END

SUBROUTINE GFIFVB(F,IA,IS,IC,VA,VB,FC)

.  
.  
.

YRG=CMPLX(1.0/RG,0.0)

C COMPUTE Y1 AND Y3 FROM VARIABLES GIVEN

IF(ABS(W).GT.0.3E8.AND.ABS(W).LT.1.E9) GO TO 119  
IF(ABS(W).LT.0.3DE8) GO TO 117

C REAL AND IMAGINARY PARTS OF Y1 AND Y3 AT HIGH FREQUENCY

Y1R=Q(1)  
Y1I=-Q(2)/W  
Y3R=Q(3)  
Y3I=-Q(4)/W  
GO TO 119

C REAL AND IMAGINARY PARTS OF Y1 AND Y3 AT LOW FREQUENCY

117 Y1R=Q(5)  
Y1I=-Q(6)/W  
Y3R=Q(7)  
Y3I=-Q(8)/W

118 CONTINUE  
Y1=CMPLX(Y1R,Y1I)  
Y3=CMPLX(Y3R,Y3I)  
GO TO 120

119 Y1=CMPLX(0.0,0.0)  
Y3=CMPLX(0.0,0.0)

120 CONTINUE

YRB=CMPLX(1.0/RB,0.0)

.  
.  
.  
.

## CHAPTER VI

### SUMMARY

This report summarizes the second phase of a study which makes use of passive compensating networks to reduce in-band nonlinear effects in electronic systems by altering the out-of-band linear responses of the system. This phase of the study emphasizes the reduction of third-order intermodulation when the interfering signals fall within certain bands of frequencies. The method used is primarily a numerical experimentation.

Several important conclusions have been reached as a result of this study. One observation is that the complexity of the compensating networks usually has little to do with the intermodulation reduction. Since more complicated networks are obviously more costly, the compensating networks used in this scheme should be as simple as possible. Since both the real part and the imaginary part play a role in the reduction, the simplest network would be an RC or an RL branch.

Based on the results obtained by this study, there is definitely a trade-off between the amount of reduction and the bandwidths of the signals. It appears that this technique is most suitable for narrow-to-medium band applications. A typical situation in which this method would be effective is when the second-order frequency affected has a 25 percent bandwidth.

A step-by-step description of the algorithm used in this study is presented in this report. The computational strategy recommended for finding the compensating network parameters is also given.

Several aspects that warrant further study are:

(1) The design of the isolation parts (the lowpass and the highpass) of the compensating network. For narrow-band situations, a simple tank circuit or a blocking capacitor will be adequate. However, for medium-band situations the design of these network is apparently a non-trivial problem. It appears that this is an area worthy of further investigation. The solution of this problem is not only useful here, it also has numerous general applications.

(2) The sensitivity and techniques of tuning the compensating networks should be studied.

(3) It would be highly desirable that the technique described in this report as applied to a practical amplifier be verified in the laboratory by direct measurement. This experimental work will not only support the usefulness of this new technique, but also give a good indication of practical difficulties that might require further study.

# REFERENCES

1. K. L. Su, Reduction of In-Band Nonlinear Effects in Electronic Systems Through the Design of Out-of-Band Linear Responses, Phase Report RADC-TR-75-30, Rome Air Development Center, Griffiss AFB, New York, February 1975, (A007777).
2. K. L. Su, D. D. Weiner, and J. F. Spina, "Reduction of In-Band Nonlinear Effects in Electronic Systems Through the Design of Out-of-Band Linear Response," Proceedings 1975 IEEE International Symposium on Circuits and Systems, pp. 293-296, Boston, Mass., April 1975.
3. J. F. Spina, K. L. Su, and D. D. Weiner, "Reduction of Circuit Intermodulation Distortion Via the Design of the Linear Out-of-Band Behavior," Presented at the 1975 IEEE International Symposium on Electromagnetic Compatibility, San Antonio, Texas, October 1975.
4. M. H. Lee, All-Tolerance Multiparameter Sensitivity and Multi-variable Continuously Equivalent Networks, Ph.D. Thesis, Georgia Institute of Technology, Atlanta, Georgia, June 1975.
5. E. S. Kuh, "Special Synthesis Techniques for Driving Point Impedance Functions," IRE Trans. on Circuit Theory, Vol. CT-2, pp. 302-308, December 1955.
6. M. E. Van Valkenburg, Introduction to Modern Network Synthesis, John Wiley and Sons, Inc., 1960.
7. S. Narayanan, "Transistor Distortion Analysis Using Volterra Series Representation," Bell System Tech. Journ., Vol. 46, pp. 991-1024, May-June 1967.
8. Signatron, Inc., Nonlinear System Modeling and Analysis with Applications to Communications Receivers, Technical Report RADC-TR-73-178, Rome Air Development Center, Griffiss AFB, New York, June 1973, (766278).
9. D. D. Weiner, RADC Seminar Notes, 1973.



# APPENDIX A

## DESCRIPTION OF SUBROUTINE CGJR

This subroutine solves simultaneous equations, computes a determinant, or inverts a matrix or any combination of the three above by using Gauss-Jordan elimination technique with column pivoting.

### Program Listing

```

SUBROUTINE CGJR(A,NC,NR,N,MC,JC,V),
  RETURNS(M1)
  DIMENSION JC(NC)
  COMPLEX CLOG,V,XC,A(NR,NC)
  COMPLEX Z
  IW=V
  V=(0.,0.)
  IBIT=0
  M=1
  L=N+(MC-N)*(IW/4)
  KD=2-MOD(IW/2,2)
  KI=2-MOD(IW,2)
  GO TO (5,20),KI
5   DO 10 I=1,N
10  JC(I)=I
20  DO 31 I=1,N
    GO TO (22,21),KI
21  M=I
22  IF (I.EQ.N) GO TO 60
    X=-1.
    DO 30 J=I,N
      ANORM=ABS(REAL(A(J,I)))+ABS(AIMAG(A(J,I)))
      IF(X.GT.ANORM) GO TO 30
      X=ANORM
      K=J
30  CONTINUE
    IF(K.EQ.I) GO TO 60
    IBIT=IBIT+1
    GO TO (35,40),KI
35  MU=JC(I)
    JC(I)=JC(K)
    JC(K)=MU
40  DO 50 J=M,L
    XC=A(I,J)
    A(I,J)=A(K,J)
    A(K,J)=XC
50  ANORM=ABS(REAL(A(I,I)))+ABS(AIMAG(A(I,I)))
60  IF(ANORM.GT.0) GO TO 70
    V=(0.,0.)
    JC(1)=I-1
    RETURN M1

```

AD-A035 855

GEORGIA INST OF TECH ATLANTA

COMPUTATIONAL TECHNIQUES FOR THE REDUCTION OF NONLINEAR EFFECTS--ETC(U)

DEC 76 K L SU

F/G 9/5

F30602-75-C-0118

UNCLASSIFIED

RADC-TR-76-369

NL

2 OF 2  
AD-A  
035 855



END  
DATE  
FILMED  
3-24-77  
NTIS

```

70 GO TO (71,72),KD
71 V=V+CLOG(A(I,I))
   Z=CLOG(A(I,I))
72 XC=A(I,I)
   A(I,I)=(1.,0.)

   DO 80 J=M,L
   A(I,J)=A(I,J)/XC
   IF(LEGVAR(A(I,J))) 150,80,150
80 CONTINUE
   DO 91 K=1,N
   IF(K.EQ.I) GO TO 91
   XC=A(K,I)
   A(K,I)=(0.,0.)
   DO 90 J=M,L
   A(K,J)=A(K,J)-XC*A(I,J)
   IF(LEGVAR(A(K,J))) 150,90,150
90 CONTINUE
91 CONTINUE
   GO TO (95,140),KI
95 DO 130 J=1,N
   IF(JC(J).EQ.J) GO TO 130
   JJ=J+1
   DO 100 I=JJ,N
   IF(JC(I).EQ.J) GO TO 110
100 CONTINUE
110 JC(I)=JC(J)
   DO 120 K=1,N
   XC=A(K,I)
   A(K,I)=A(K,J)
120 A(K,J)=XC
130 CONTINUE
140 JC(1)=N
   V=V+(0.,3.14159265)*CMPLX(FLOAT(MOD(IBIT,2)),0.)
   RETURN
150 JC(1)=1-I
   RETURN M1
END

```

### Program Description

- A is the matrix whose inverse or determinant is to be determined. If simultaneous equations are solved, the last MC - N columns of the matrix are the constant vectors of the equations to be solved. On output, if the inverse is computed, it is stored in the first N columns of A. If simultaneous equations are solved, the last MC - N columns contain the solution vectors.
- NC is the maximum number of columns of the array A.
- NR is the maximum number of rows of the array A.
- N is the number of rows of the array A.
- MC is the number of columns of the array A. This entry is a dummy argument, if simultaneous equations are not to be solved.
- K is a statement number in the calling program to which control is returned if an overflow is detected. It must be preceded by \$ in the calling sequence.
- JC is a one-dimensional permutation array of N elements used for permuting the rows and columns of A if an inverse is computed. If an inverse is not computed this argument must have at least one cell for the error return identification. On output, the first element of the array is N if control is returned normally. If an overflow is detected, the first element is the negative of the last correctly completed row of the reduction. If matrix singularity is detected, the entry contains the value of the last row before the singularity was detected.
- V on input REAL (V) is the option indicator, its values are set as follows:

OPERATION	REAL (V)						
	1.	2.	3.	4.	5.	6.	7.
Compute Determinant	no	yes	yes	no	no	yes	yes
Invert Matrix	yes	no	yes	no	yes	no	yes
Solve Equations	no	no	no	yes	yes	yes	yes



# *MISSION of Rome Air Development Center*

*RADC plans and conducts research, exploratory and advanced development programs in command, control, and communications (C<sup>3</sup>) activities, and in the C<sup>3</sup> areas of information sciences and intelligence. The principal technical mission areas are communications, electromagnetic guidance and control, surveillance of ground and aerospace objects, intelligence data collection and handling, information system technology, ionospheric propagation, solid state sciences, microwave physics and electronic reliability, maintainability and compatibility.*

